INFORMATION TO USERS

This manuscript has been reproduced from the microfilm master. UMI films the text directly from the original or copy submitted. Thus, some thesis and dissertation copies are in typewriter face, while others may be from any type of computer printer.

The quality of this reproduction is dependent upon the quality of the copy submitted. Broken or indistinct print, colored or poor quality illustrations and photographs, print bleedthrough, substandard margins, and improper alignment can adversely affect reproduction.

In the unlikely event that the author did not send UMI a complete manuscript and there are missing pages, these will be noted. Also, if unauthorized copyright material had to be removed, a note will indicate the deletion.

Oversize materials (e.g., maps, drawings, charts) are reproduced by sectioning the original, beginning at the upper left-hand corner and continuing from left to right in equal sections with small overlaps.

ProQuest Information and Learning
300 North Zeeb Road, Ann Arbor, MI 48106-1346 USA
800-521-0600

Desalination by membrane distillation

a comparative study of tubular and hollow fibre membrane units

by
Ludovic Plasse

Department of Chemical Engineering
McGill University, Montreal
November, 2000

A thesis submitted to the Faculty of Graduate Studies and Research in partial fulfilment of the requirements of the degree of Master of Engineering

À mes Grands-Parents, à mes Parents et à mes Frères

To my Grandparents, Parents and Brothers

Abstract

Membrane distillation was considered as an alternative to traditional desalination processes because this technique produces ultra-pure water without requiring high temperatures nor high pressures.

The driving force of membrane distillation is a temperature difference across a microporous membrane leading to a vapour pressure gradient. Hydrophobic membranes are used for membrane distillation in order to permit the passage of vapours through the pores while preventing the liquid phase from passing.

The thickness of the membrane is a key variable which affects heat and mass transfers between the warm feed side and cooling side. In this thesis, a module with thin-walled hollow fibres was compared to a module with thicker tubular membranes. The permeate flux produced was compared at different operating conditions. Feed and cooling water flow rates and temperatures were varied. The impact of salt concentration in the feed was also examined.

Different models based on first principles were developed and compared to a semi-empirical model based on the experimental determination of the mass transfer coefficient. Their predictions were compared with experimentally obtained permeate fluxes.

Résumé

La distillation membranaire est une possible alternative aux méthodes classiques de dessalement car elle permet de produire une eau extrêmement pure sans avoir recours à des températures ou à des pressions élevées.

Le principe de la distillation membranaire repose sur l'établissement d'une différence de température entre les deux faces d'une membrane microporeuse créant ainsi un gradient de pression de vapeur. Les membranes hydrophobes utilisées permettent alors le passage de vapeurs au travers des pores mais empêchent tout liquide de traverser.

L'épaisseur de la membrane est un paramètre clef affectant les transferts de masse et de châleur entre les côtés chaud et froid. Dans cette thèse, un module composé de fines fibres creuses a été comparé à un module composé de tubes creux plus épais. Les flux de perméat ont été comparé pour différentes conditions opératoires en variant les températures et les débits des eaux d'alimentation et de refroidissement. L'impact de la concentration en sels dans l'eau d'alimentation a de même été examiné.

Différents modèles basés sur les premiers principes ont été developpés et comparés à un modèle semi-empirique basé sur la détermination expérimentale du coefficient de transfert de masse. Leurs prédictions ont été comparées avec les résultats expérimentaux obtenus pour les flux de perméat.

Acknowledgements

I would like to express my gratitude to my supervisor Professor Jana Simandl for her guidance and support. I greatly appreciated her suggestions throughout the research. Thank you very much Professor Simandl.

The financial support of the Max Stern Scholarship was gratefully appreciated and gave me the chance to do this research.

Thanks to my research group and to the staff of the Chemical Engineering Department. Lou Cusmich for his computer and data acquisition assistance, Alain Gagnon and Frank Caporuscio for their technical assistance. Frank, your advises and help were greatly appreciated. In the future, I might support the Italian soccer team !

Table of contents

List of figures

List of tables

Nomenclature

Symbols

C	Membrane mass transfer coefficient
c	Molecular concentration
d	diameter
D	Diffusion coefficient
J	Mass flux of permeate
K	Mass transfer coefficient
k	Thermal conductivity
M	Molecular mass
N	Molar flux of permeate
n	Number of segments in model
P	Pressure
P'	Pressure
Q	Heat transfer
r	Radius
T	Temperature
v	Atomic diffusion volume
x	Mole fraction
z	Direction of the flow

Greek Letters

δ	Thickness
ε	Porosity of the membrane
λ	Mean free path
μ	Viscosity
ρ	Density
τ	Tortuosity of the membrane
ψ	Latent heat of vaporisation
ζ	Polarisation coefficient

Subscripts

A	Air
A1	Air at the entrance of the pore
A2	Air at the exit of the pore
b1	Feed bulk
b2	Cooling water bulk
bs	Salt in the bulk feed
c	Conductive
g	Gas phase
h	Hydraulic
m	Membrane
m1	Feed side membrane surface
m2	Cooling side membrane surface
ms	Salt at the membrane surface
p	Polarisation layer
s	Salt
solid	Solid phase
v	Vapour
vapo.	Vaporisation
W	Water vapour
W1	Water vapour at the entrance of the pore
W2	Water vapour at the exit of the pore

Dimensionless Numbers

Kn	Knudsen Number
Nu	Nusselt Number
Pr	Prandl Number
Re	Reynolds Number
Sc	Schmidt Number

1 Introduction

Distillation/evaporation and reverse osmosis are the two major techniques currently used for sea water desalination. These processes are expensive because of important heat and pressure requirements. Membrane distillation may prove to be a viable alternative.

While establishing the feasibility of membrane distillation at McGill University's Chemical Engineering Department, flat sheets and tubular membranes were used for the production of fresh water from sea water and for the purification of water contaminated by volatile organic compounds such as benzene, ethanol and acetone [1-3].

One of the key parameters in membrane distillation is the thickness of the membrane. A thicker membrane slows down both heat transfer, which is an advantage, and also mass transfer, which is obviously a disadvantage for the process. Globally, the impact on mass transfer is expected to supersede that on the heat transfer. Thus, thin flat-sheet membranes have an advantage over thicker tubular units. Unfortunately, it is difficult to scale-up flat sheet membranes. A third alternative, and the purpose of this thesis, is to use hollow fibre membranes which combine the advantages of both, a small membrane thickness (three times thinner than the tubular membranes) and a scale-up capability. It was expected that the flux per unit area would increase dramatically with hollow fibre membranes compared to tubular ones.

A literature review of membrane distillation and its application to desalination and to other separation and concentration processes is presented in chapter 2. Semi-empirical and theoretical models are developed in chapter 3. The description of the apparatus and of the experimental procedure follows in chapter 4. The experimental results are discussed in chapter 5. In chapter 6, conclusions are drawn and recommendations made.

2 Literature review

2.1 Membrane distillation

Membrane distillation is a membrane process whose selectivity is based upon vapour pressure differences. The process was first studied in the sixties [4] and provides an interesting alternative to other desalination processes such as reverse osmosis and distillation/evaporation. Membrane fouling is less important in membrane distillation than for conventional membrane processes and an almost perfect rejection of ions, macromolecules, colloids, cells and other non-volatile components is achieved. Moreover, the operating temperatures (30 to 90°C) and pressures (atmospheric to a few hundreds kPa) result in lower costs with the possible exception of vacuum membrane distillation [5].

Capillary distillation and trans-membrane distillation are different terms used to designate membrane distillation. Since 1986 and the "Workshop on Membrane Distillation" in Rome, the process has been defined as one which should exhibit the following characteristics :

- The membrane should be porous,
- The membrane should not be wetted by the process liquids,
- No capillary condensation should take place inside the pores of the membrane,
- The membrane should not alter the liquid-vapour equilibrium of the different components in the process liquids,
- At least one side of the membrane should be in direct contact with the process liquid.

The driving force of membrane distillation is the vapour pressure difference across the hydrophobic porous membrane whose surfaces are held at different temperatures. The

liquid water phase cannot pass through the hydrophobic membrane whereas water vapours can. The volatile components (water in desalination) diffuse from the warmer side (feed side), to the cooler side (permeate side), and condense. The limitation of the process is the risk of membrane wetting. This places a limit on the upper concentration of any surface active components permitted within the feed.

Four different configurations can be used for membrane distillation (Figure 2.1) : direct contact membrane distillation, air gap membrane distillation, vacuum membrane distillation and sweep gas membrane distillation [1-3,5,6]. In air gap, sweep gas and vacuum membrane distillation, the cooling surface is separated from the membrane by, respectively, an air gap, an inert gas which collects the vapours or a vacuum which draws out the vapours from the permeate side [1-3,5,6]. In direct contact membrane distillation, a cooling liquid is in contact with the membrane surface and the vapours which pass through the pores condense within it. The operation is simple and it requires the least equipment [5]. This configuration is the one used throughout all the experiments performed as part of this thesis.

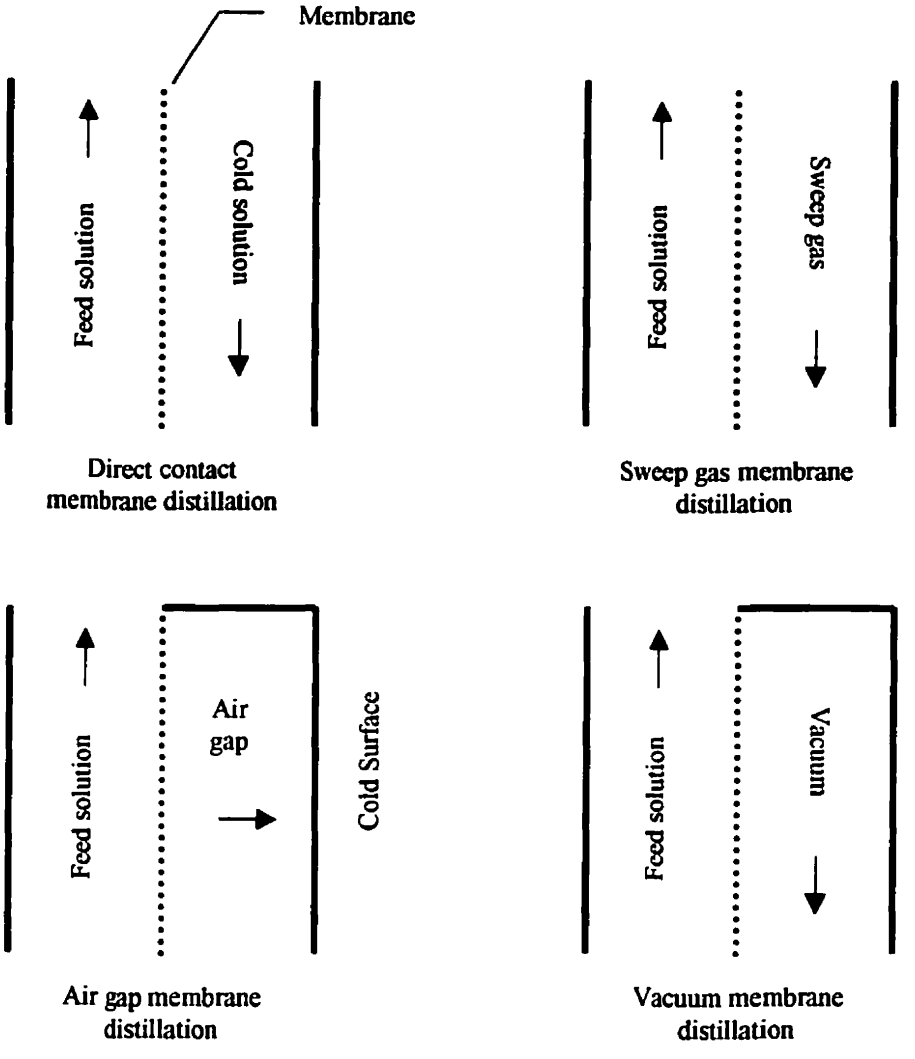

Figure 2.1 : Different configurations for membrane distillation [5]

2.2 Membrane distillation for desalination

Because of the very high quality of the water produced by membrane distillation, a possible application of this process is the production of drinking water from sea water. Direct contact membrane distillation is the most appropriate configuration for desalination [5] and was used for the experiments (Figure 2.2).

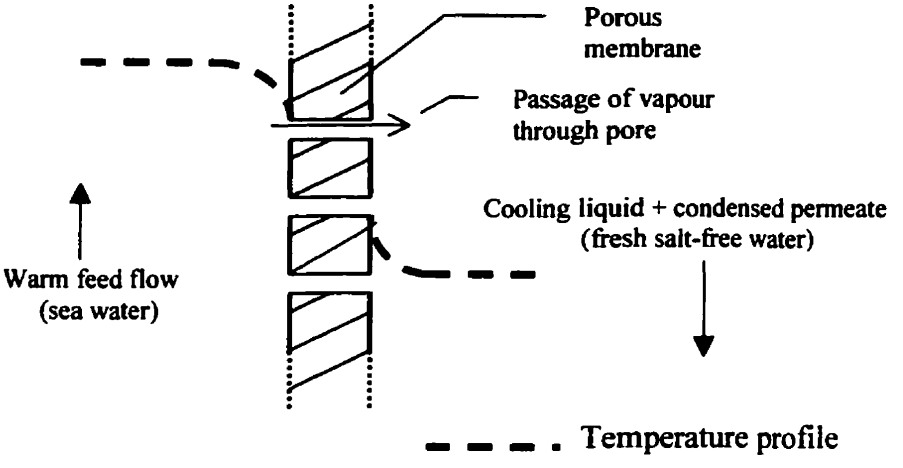

Figure 2.2 : Direct contact membrane distillation

Fawzi Banat [1] studied desalination by air gap membrane distillation with flat sheet membranes while Stéphanie Lacoursière [2] and Praveen Ram Menta Prasanna [3] investigated the effects of different factors on direct contact membrane distillation. First, Banat [1] and Lacoursière [2] observed that the salt concentration has little effect on the permeate flux up to five percent by weight salt. Secondly, all three observed that increasing the feed flow rate in the laminar region increased the permeate flux because of the reduction in temperature and concentration polarisation. Once turbulent flow was established, changes in permeate flux were negligible. Thirdly, the temperature difference between the feed side and the permeate side had an important effect on the permeate flux : flux increased with an increase in temperature difference. And lastly, they noted that the temperature of the feed side had a large effect on the permeate flux.

The higher the feed side temperature is, the higher the flux. Two similar semi-empirical models for heat and mass transfer were proposed by Lacoursière [2] and Prasanna [3] and will be used in this work.

2.3 Membrane distillation for applications other than desalination

Membrane distillation could be useful in different industrial processes but most of the applications are still at the laboratory scale and have not been evaluated on a larger scale. One application in the food industry is the concentration of aqueous solutions such as fruit juices or milk. F. Laganà, G. Barbieri and E. Drioli [7] used direct contact membrane distillation with polypropylene hollow fibre modules MD-020-2N-CP from ENKA Microdyn to produce a highly concentrated apple juice (64°Brix). Their results were good but they did not compare the economics of this technique with traditional evaporation.

M. Tomaszewska [8] found that direct contact membrane distillation could be applied for the separation and concentration of fluosilicic acid during the production of phosphoric acid by a wet process. The module used was a plate and frame module with a PVDF membrane. A fluosilicic acid distillate, almost free of phosphoric acid, was obtained at a higher concentration than that of the feed.

Membrane distillation has also a lot of possible environmental applications such as the concentration of radioactive components in liquid low-level radioactive waste. This was studied by G. Zakrzewska-Trznadel, M. Harasimowicz and A.G. Chmielewski [9]. A pilot plant with a spiral-wound PTFE membrane of $4m^2$ distillation area was used. A distillate production of 0.05 m^3/h with a radiochemical purity of less than 10 Bq/dm^3 for β and γ emitters was achieved. Moreover, this process avoided many problems encountered in normal evaporation (corrosion, scaling or foaming) or with other membrane processes (fouling, sorption of radioactive ions, high pressure). A preliminary economic analysis has shown that membrane distillation is advantageous for low capacity plants if waste heat is used.

Another environmental application is the processing of liquid photographic waste. K.B. Grekov and V.E. Senatorov [10] used direct contact membrane distillation with a fluoroplastic membrane and found that this process has a high efficiency and is competitive with other membrane processes such as reverse osmosis. Moreover, a high degree of concentration could be achieved without affecting the retention capacity. The energy requirement to heat the feed is low because of the high temperature of the effluent (27-43°C).

Membrane distillation could also be applied to the separation of water and glycols. C. Rincón, J.M. Ortiz de Zárate, J.I. Mengual [11] investigated direct contact membrane distillation, with three different PTFE flat sheet membranes, as a possible technology for the concentration of used coolant liquids containing ethylene glycol. A high concentration (70%) of ethylene glycol could be achieved by using moderate temperatures and atmospheric pressure. This process could be competitive if waste heat is used to pre-heat the feed.

M. Gryta and K. Karakulski [12] applied direct contact membrane distillation with a polypropylene capillary membrane to the concentration of oil-water emulsions. The authors achieved an almost perfect separation with a feed concentration up to 1000 ppm. The oil concentration of the feed was maintained below 1000 ppm by removing the oil phase formed by the emulsion breaking.

A potential application in drinking water treatment is the removal of volatile organic compounds. N. Couffin, C. Cabassud and V. Lahoussine-Turcaud [13] studied the removal of halogenated VOCs (chloroform, trichloroethylene, tetrachloroethylene) at a very low concentration by vacuum membrane distillation with a flat PVDF membrane from Millipore S.A.. They concluded that the process is an efficient and economical technology to remove volatile halogenated organic compounds at low concentrations in drinking water.

F. A. Banat and J. Simandl [14,15] studied the air gap membrane distillation as a possible method for the removal of propanone and ethanol from aqueous solutions. The membranes used were polyvinyldene fluoride (PVDF) flat sheets from Millipore. In another study [16], the authors evaluated the benzene removal by vacuum membrane distillation with a tubular polypropylene membrane module. They found that this process is competitive with the traditional air-stripping tower provided that comparable contact areas are used. An additional advantage is that the benzene is captured rather than merely diluted in an air stream.

3 Modelling

There have been two approaches taken for the modelling of membrane distillation. A rigorous one which focuses on the transport mechanisms through the membrane, and a semi-empirical approach for predicting the permeate flux at given operating conditions [17]. For both, the general expression of the mass flux J is usually given by equation (3.0) [2-3,5,6,18,19] :

$$J = C \cdot (P_{m1} - P_{m2}) \qquad (3.0)$$

Where P_{m1} and P_{m2} are the vapour pressures of the feed side and the cooling side respectively. C is the mass transfer coefficient which is a strong function of the membrane used (pore size, porosity, thickness) [18] and of the flow rates on both sides of the membrane. C could be determined either experimentally (semi-empirical model) [2,3,8,18,20] or theoretically (Knudsen diffusion, molecular diffusion, Hagen-Poiseuille viscous flow) [5,6,17]. Both models are of interest; the semi-empirical for the comparison of existing units scale-up and the theoretical for improving the understanding of what is happening. Both are described in this chapter and used in chapter 5.

In both cases, to predict the permeate flux in membrane distillation, heat and mass transfer rates should be evaluated. These transfers are inter-related and are extensively discussed in the literature [5,6,17-22]. The main modelling problem is the appearance of temperature and concentration polarisation on both sides of the membrane as shown in Figure 3.1. The values of the membrane surface temperatures are unknown and depend upon the estimation of the boundary layer thickness. The semi-empirical models incorporate the polarisation effects into a membrane constant which is a function of the flow conditions. The theoretical models strive to predict the polarisation from first principles.

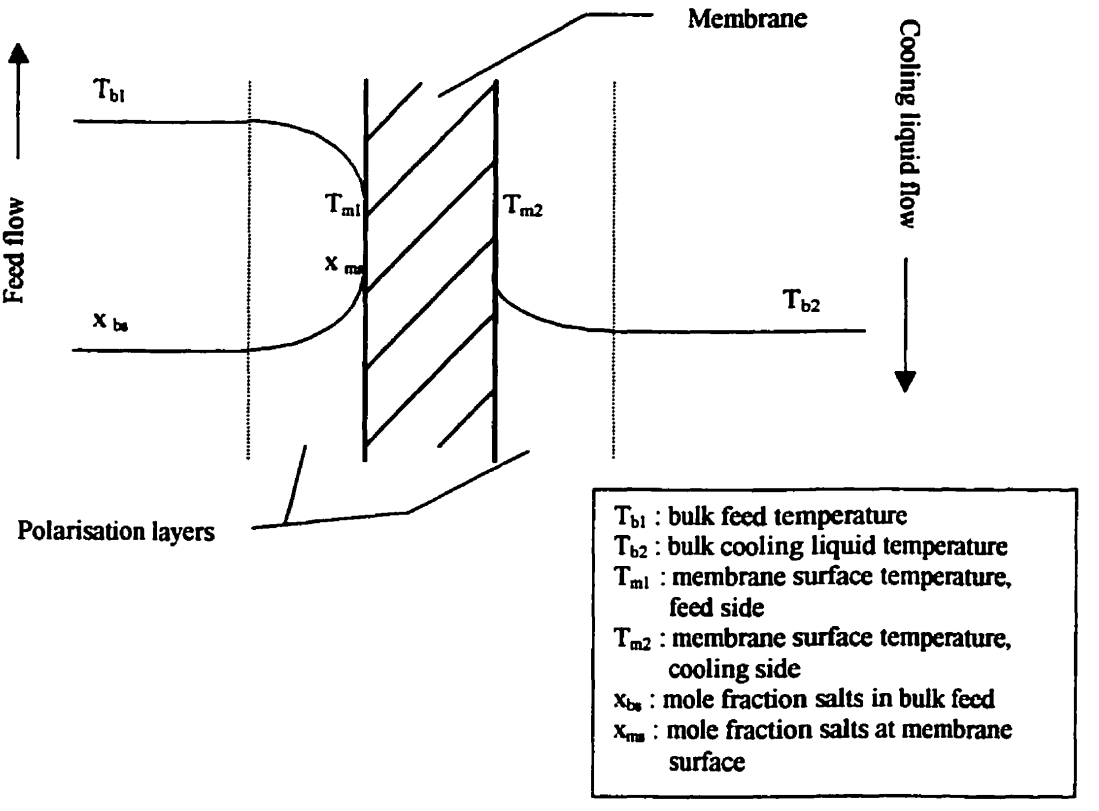

Figure 3.1 : Temperature and concentration polarisation layers

3.1 Semi-empirical approach

The semi-empirical approach successfully predicted the permeate flux for the tubular membranes used by Lacoursière [2] and Prasanna [3]. It was the starting point for the modelling of the hollow fibre membrane in this thesis. Other similar semi-empirical models were developed in the literature and showed a good correlation with their respective experimental conditions [5,6,17-21].

Equation (3.0), expressed previously, gives the mass flux, J, through the membrane as a function of the membrane mass transfer coefficient, C, and of the vapour pressure difference.

The vapour pressure can be calculated using Antoine's equation:

$$P_v = \exp\left[B - \frac{A}{(D+T)}\right] \qquad (3.1.0)$$

Where P_v is the vapour pressure in Pascal, T is the temperature in Kelvin, and A,B and D are experimental constants. For water, A=3841, B=23.238 and D=-45.

Any decrease in the vapour pressure due to the salt concentration is accounted for by using Raoult's law :

$$P' = (1 - x_{ms}) \cdot P \qquad (3.1.1)$$

Where P is the vapour pressure of pure water, P' is the vapour pressure of the water with salt, and x_{ms} is the mole fraction of the salt at the membrane surface.

Since concentration polarisation occurs, the mole fraction of the salt at the membrane surface is not the same as in the bulk. The salt concentration at the surface of the membrane could then be calculated using the film model :

$$c_{ms} = c_{bs} \cdot \exp\left(\frac{J}{\rho K_s}\right) \qquad (3.1.2)$$

Where c_{ms} and c_{bs} are respectively the salt concentration at the surface of the membrane and in the bulk, ρ is the density of the bulk and K_s is the salt mass transfer coefficient.

K_s could be evaluated by employing the Dittus-Boelter correlation :

$$K_s = 0.023 \cdot \mathrm{Re}^{0.8} \cdot Sc^{0.33} \cdot \frac{D_{WA}}{d_h} \qquad \textit{(3.1.3)}$$

Where Re is the Reynolds number, Sc is the Schmidt number, D_{WA} is the diffusion coefficient of water vapour through stagnant air (~$2.6*10^{-5}$ m^2/s at 30°C) and d_h is the hydraulic diameter (m).

The diffusion coefficient D_{WA} (m^2/s) of water vapour in stagnant air is given by the Fuller and al. equation [23] :

$$D_{WA} = \frac{0.01013 \cdot T^{1.75} \cdot \left(\frac{1}{M_W} + \frac{1}{M_A}\right)^{1/2}}{P \cdot \left(v_W^{1/3} + v_A^{1/3}\right)^2} \qquad \textit{(3.1.4)}$$

Where T is the temperature in Kelvin, P the pressure in Pascal, M_W and M_A the molecular masses of water and air, v_W and v_A the atomic diffusion volumes (20.1 for air and 12.7 for water) [23].

The temperatures at the surfaces of the membrane (T_{m1} and T_{m2}) are necessary to calculate the permeate flux taking into account the temperature polarisation. Evaluating the heat transfer through the membrane will provide these temperatures. The heat transfer (Q) is the sum of the conductive (Q_c) and vaporisation ($Q_{vapo.}$) heat transfers [2-3,5,6,17,18,20,21] :

$$Q_c = \frac{k_m}{\delta_m} \cdot (T_{m1} - T_{m2}) \qquad (3.1.5)$$

$$Q_{vapo.} = N \cdot \psi \qquad (3.1.6)$$

$$Q = Q_c + Q_{vapo.} = \frac{k_m}{\delta_m} \cdot (T_{m1} - T_{m2}) + N \cdot \psi \qquad (3.1.7)$$

Where ψ is the latent heat of vaporisation, δ_m is the thickness of the membrane, N the molecular flux of water through the membrane and k_m is the thermal conductivity of the membrane :

$$k_m = \varepsilon \cdot k_g + (1 - \varepsilon) \cdot k_{solid} \qquad (3.1.8)$$

Where k_g and k_{solid} are the thermal conductivity of the gas phase and of the solid phase respectively. ε is the porosity of the membrane [18].

Q is also equal to the heat flux through the polarisation layer :

$$Q = \frac{k_p}{\delta_p} \cdot (T_{b1} - T_{m1}) = \frac{k_p}{\delta_p} \cdot (T_{b2} - T_{m2}) \qquad (3.1.9)$$

δ_p is the thickness of the polarisation layer and k_p is its thermal conductivity.

Manipulating (3.1.7) and (3.1.9) gives T_{m1} and T_{m2} so the vapour pressure at the surfaces of the membrane could be calculated and then the permeate flux.

The polarisation coefficient, ζ, is then defined as [18] :

$$\zeta = \frac{T_{m1} - T_{m2}}{T_{b1} - T_{b2}} \qquad \textit{(3.1.10)}$$

3.2 Computer Modelling

Based on the program written by Lacoursière and Prasanna in FORTRAN, a Visual Basic program was written under Microsoft Excel (Appendix A). This program was based on the semi-empirical model described above, using physical characteristics of the modules and an experimental estimation of the mass transfer coefficient C at given flow rates on both sides of the membrane. A Windows interface has been created to easily get the predicted permeate flux by entering the entrance temperatures of the feed and of the cooling water, their flow rates and the salt concentration (Figure 3.2).

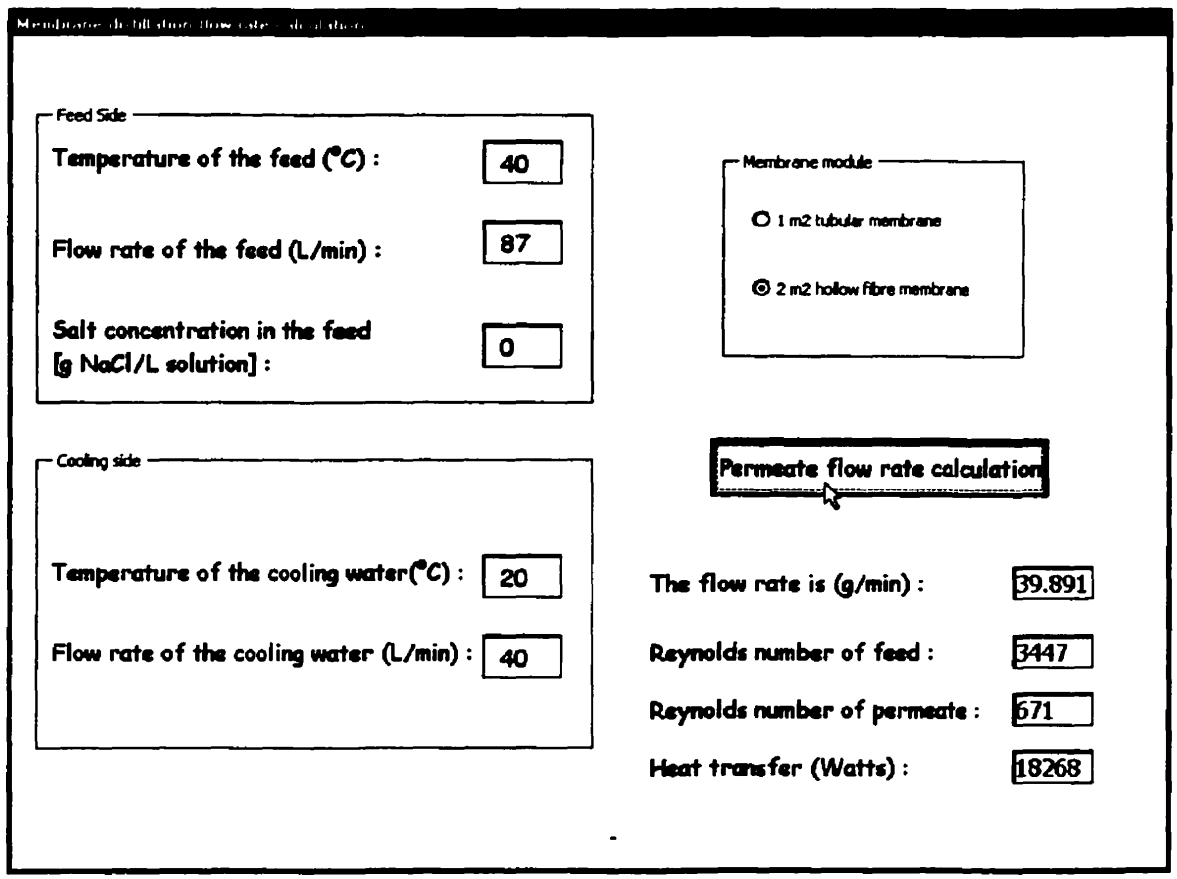

Figure 3.2 : Screen capture of the interface

For the calculations, the module is divided into n segments and the water flux is computed iteratively for each segment (Figure 3.3). The exit cooling temperature is first set at twenty degrees celsius and an iteration is then performed to calculate the permeate flux through the first segment.

The temperatures of the feed and of the cooling water are then calculated for the next segment by assuming that the total heat is transferred from the previous segment. At the last segment, the calculated cooling water temperature is compared with the actual one. If the difference is greater than the maximum acceptable difference, the calculation is repeated from the first segment with an updated entrance cooling water temperature. The segment permeate fluxes are then added to give the total permeate flux through the membrane.

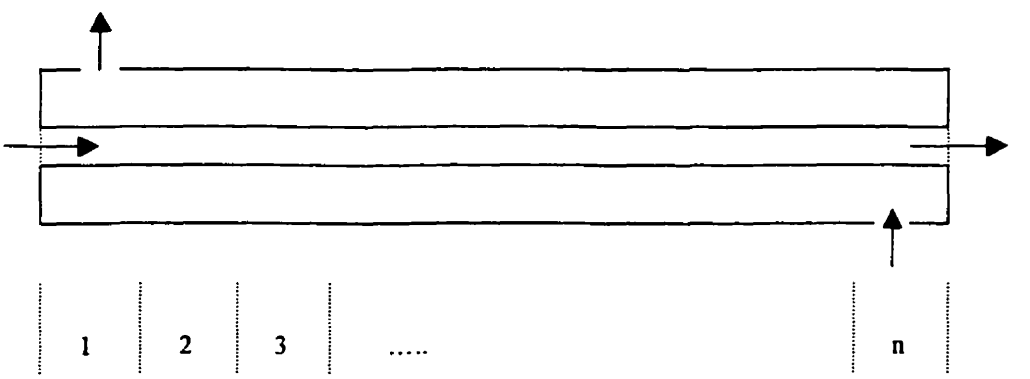

Figure 3.3 : Division of a membrane module in n segments

As will be seen in chapter 5, the predictions of the model compared very well with the experimental values for both distilled water and a saline solution.

3.3 Theoretical determination of the membrane mass transfer coefficient

Based on the mean free path of water molecules, three theoretical approaches are used in literature to estimate the membrane mass transfer coefficient C : Knudsen diffusion, molecular diffusion and Hagen-Poiseuille viscous flow. If the mean free path

is very long compared to the pore size, Knudsen diffusion is deemed to happen and the diffusion takes place by a series of collisions between the water molecules and the membrane walls. At the opposite extreme, if the mean free path is very short compared to the pore size, molecular diffusion is deemed to happen by a series of collisions between the molecules. For very wide pores compared to the mean free path, Hagen-Poiseuille relation could be used.

For water, the mean free path, λ, could be calculated as follow :

$$\lambda = 3 \cdot \frac{\mu}{P} \cdot \left(\frac{\pi RT}{8M} \right)^{1/2} \qquad \textit{(3.2.0)}$$

Where μ (Pa.s) is the viscosity of the water vapour at a pressure P (Pa) and a temperature T (K). M is the molecular mass of water ($kg.mol^{-1}$) and R the gas constant ($8.314\ J.K^{-1}.mol^{-1}$).

The predominant mechanism is determined by calculating the Knudsen number Kn :

$$K_n = \frac{\lambda}{d} \qquad \textit{(3.2.1)}$$

Where d is the mean diameter of the membrane pores.

For Kn less than 0.01, the pore diameter is very large compared to the mean free path and molecular diffusion takes place. If Kn is greater than 10, the mean free path is much larger than the pore diameter and Knudsen diffusion is the dominant mechanism. Between 0.01 and 10 is the transition region where both transport mechanisms occur.

The Hagen-Poiseuille relation is generally applied to newtonian fluids at fully developed laminar flow in a conduit.

The Knudsen diffusion equation is the following [6,24-26] :

$$J = \frac{2}{3} \cdot \frac{r\varepsilon}{\tau} \cdot \left(\frac{8M}{\pi RT} \right)^{1/2} \cdot \frac{\Delta P_v}{\delta_m} \qquad (3.2.2)$$

Where r is the pore mean radius, τ is the tortuosity of the pores and δ_m the thickness of the membrane.

The molecular diffusion is described by Fick's First Law :

$$N_W = x_W (N_W + N_A) - cD_{WA} \nabla x_W \qquad (3.2.3)$$

Where N_W and N_A are the molar fluxes of water vapour and air, x_W is the mole fraction of water vapour, D_{WA} is the diffusion coefficient of water vapour in air and c is the molar density.

A derivation of Fick's First Law for the diffusion through a stagnant gas film is given by Stefan's equation [1,27]:

$$N_W = \frac{-cD_{WA}}{1 - x_W} \cdot \frac{dx_W}{dz} \qquad (3.2.4)$$

with,

$$c = \frac{P}{RT} \qquad (3.2.5)$$

Where P is the total pressure, R the gas constant and T the temperature.

Replacing c in equation (3.2.4) by equation (3.2.5) gives :

$$N_W = \frac{-PD_{WA}}{RT(1-x_W)} \cdot \frac{dx_W}{dz} \qquad (3.2.6)$$

At steady state, the molar flux is constant :

$$\frac{dN_W}{dz} = 0 \qquad (3.2.7)$$

So, with equation (3.2.4) :

$$\frac{d\left(\frac{-cD_{WA}}{1-x_W} \cdot \frac{dx_W}{dz}\right)}{dz} = 0 \qquad (3.2.8)$$

Considering that the gas mixture is ideal, so that c is constant, and that D_{WA} is almost independent of the concentration gives :

$$\frac{d\left(\frac{1}{1-x_W} \cdot \frac{dx_W}{dz}\right)}{dz} = 0 \qquad (3.2.9)$$

A first integration gives :

$$\frac{1}{1-x_W} \cdot \frac{dx_W}{dz} = C_1 \qquad (3.2.10)$$

A second integration gives :

$$-\ln(1-x_W) = C_1 \cdot z + C_2 \qquad (3.2.11)$$

So,

$$x_W = 1 - \exp(-C_1 \cdot z - C_2) \qquad (3.2.12)$$

And,

$$\frac{dx_W}{dz} = C_1 \cdot \exp(-C_1 \cdot z - C_2) \qquad (3.2.13)$$

Replacing in equation (3.2.6) gives :

$$N_W = \frac{-PD_{WA}}{RT(1-x_W)} \cdot C_1 \cdot \exp(-C_1 \cdot z - C_2) \qquad (3.2.14)$$

Using (3.2.12) for $z = 0$ ($x_W = x_{W1}$),and for $z = \delta_m$ ($x_W = x_{W2}$):

$$C_1 = \frac{\ln x_{A1} - \ln x_{A2}}{\delta_m} \qquad (3.2.15)$$

$$C_2 = -\ln x_{A1} \qquad (3.2.16)$$

So, with equation (3.2.14) :

$$N_W = \frac{PD_{WA}}{RTx_A\delta_m} \cdot \ln\left(\frac{x_{A2}}{x_{A1}}\right) \cdot x_{A1} \cdot \exp\left(\frac{\ln(x_{A2}/x_{A1}) \cdot z}{\delta_m}\right) \qquad (3.2.17)$$

At steady state, N_W is constant. So, calculating N_W for $z = 0$ or $z = \delta_m$ gives the molar flux through the membrane :

$$N_W = \frac{PD_{WA}}{RT\delta_m} \cdot \ln\left(\frac{x_{A2}}{x_{A1}}\right) \qquad \textit{(3.2.18)}$$

With, $x_{A1} = \frac{(P - P_{v1}) \cdot V}{RT}$

And, $x_{A2} = \frac{(P - P_{v2}) \cdot V}{RT}$

$$N_W = \frac{D_{WA} P \ln\left(\frac{P - P_{v2}}{P - P_{v1}}\right)}{RT\delta_m} \qquad \textit{(3.2.19)}$$

Taking into account the porosity and the tortuosity, finally gives the molar flux N_W through $1 m^2$ of membrane :

$$N_W = \frac{\varepsilon D_{WA} P \ln\left(\frac{P - P_{v2}}{P - P_{v1}}\right)}{RT\delta_m \tau} \qquad \textit{(3.2.20)}$$

In the case of a very large pore size compared to the mean free path, the mass flux could also be calculated by using the Hagen-Poiseuille relation [1,6,25-27] :

$$J = \frac{r^2 \varepsilon M P}{8\mu RT\delta_m \tau} \cdot \Delta P_v \qquad \textit{(3.2.21)}$$

4 Experimental apparatus and procedure

4.1 Membrane modules

Two membrane modules manufactured by Enka-Microdyn were used to conduct experiments. One was a hollow fibre unit and the other a tubular membrane unit used previously by Prasanna [3]. The characteristics of the two units are summarised in Table 4.1. It is important to note that these membranes were not designed for membrane distillation but for cross-flow microfiltration. It is the hydrophobicity of polypropylene which allows them to be used for membrane distillation. The hydrodynamics of the units were not optimised for membrane distillation. Indeed, the circulation of the cooling fluid around the membranes is inadequate (Figures 4.1 and 4.2). This particular point will be discussed in section 5.3.3.

4.2 Description of the apparatus

The experimental apparatus was almost the same for both membrane modules (Figure 4.3). The only difference was the addition of a more powerful pump and of a bigger flow meter on the permeate side for the hollow fibre unit. The modules were slightly inclined (~5%) to allow the air present on the permeate side to be purged. The cooling water was then in contact with the total membrane area.

The pressure gauges were Bourdon gauges ranging from 0 to 15 psig (0-103 kPa). The temperatures were monitored with T-type thermocouples connected to a data-acquisition system (described in section 4.3). The conductivity was read on an Omega CDW-75 conductivity meter ranging from 0 to 200 mS.

As the cooling capacity of the cooling bath was not enough, two extra immersion coolers were used when needed.

A complete list of the equipment is given in Table 4.2.

Table 4.1 : Membrane unit characteristics

	Tubular module	**Hollow fibre module**
Model type	MD 090 TP 2N ANSI	MD 080 CS 2N
Membrane area	**1 m²**	**2 m²**
Number of membranes	41	450
Nominal module diameter	9 cm	8 cm
Module length	1.5 m	1 m
Membrane inner diameter	5.5 mm	1.8 mm
Membrane outer diameter	8.5 mm	2.6 mm
Membrane thickness	**1.5 mm**	**0.4 mm**
Membrane porosity	**75%**	**75%**
Average pore size (determined by manufacturer)	**0.2 μm**	**0.2 μm**
Maximum operating temperature (specified by manufacturer)	**60°C**	**40°C**
Membrane material	Polypropylene	Polypropylene
Outer shell material	Polypropylene	Stainless Steel
Potting material	Polyurethane	Polyurethane

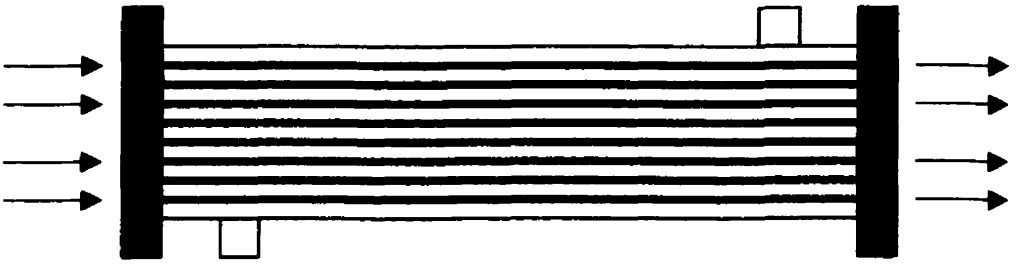

Side view

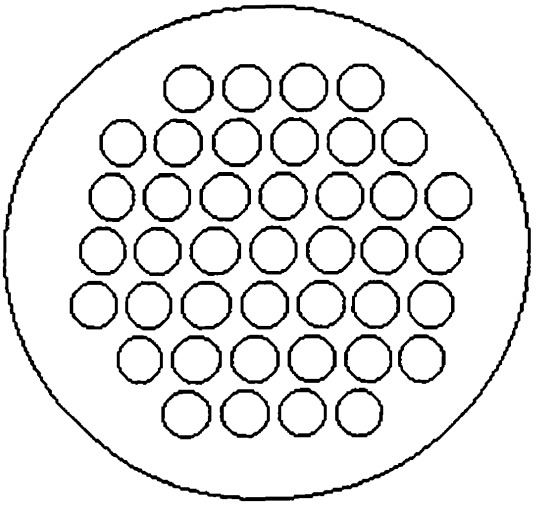

Cross section

Figure 4.1 : Tubular module

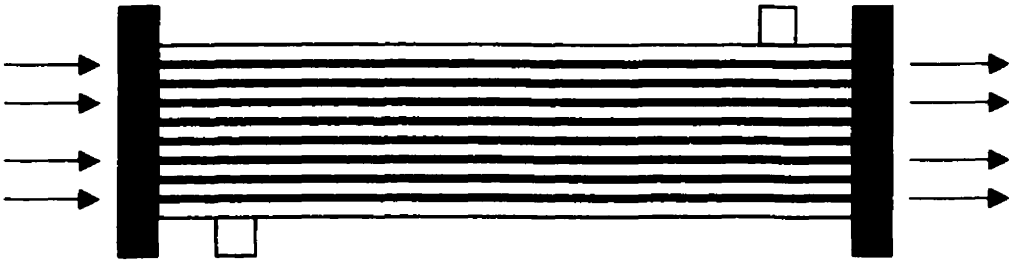

Side view

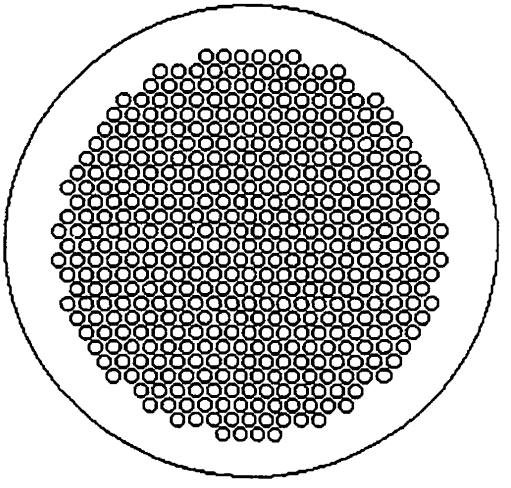

Cross section

Figure 4.2 : Hollow fibre module

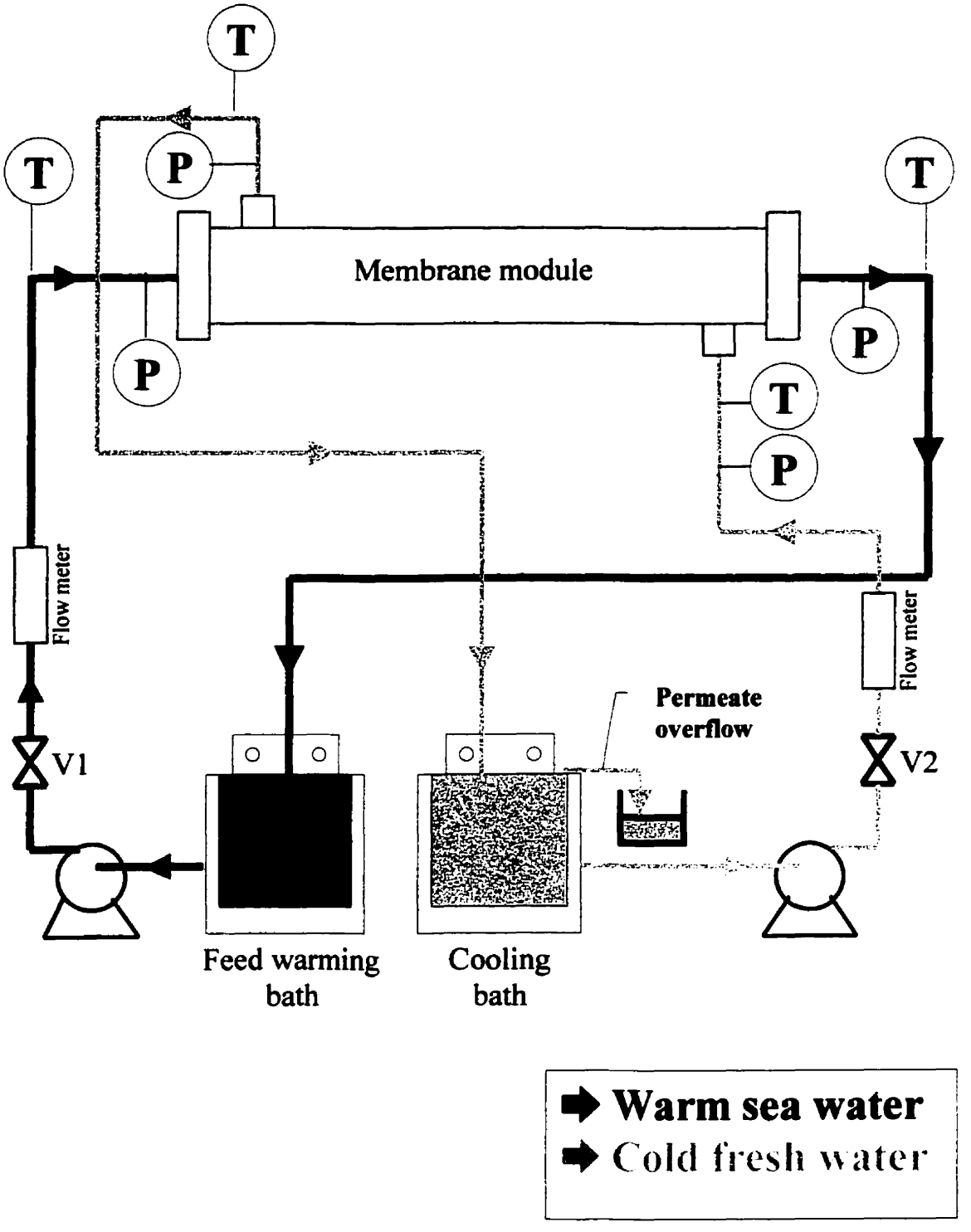

Figure 4.3 : Schematic of apparatus

Table 4.2 : List of the apparatus

Apparatus	Tubular / hollow fibre unit
Membrane	MD090TP2N / MD080CS2N
Constant temperature heating bath	Neslab GP-500
Constant temperature cooling bath	Neslab RTE-220
Immersion cooler 1	Neslab PBC-II
Immersion cooler 2	Neslab U-COOL
Feed circuit pump	Little Giant TE-7MD-HC (centrifugal, magnetic drive)
Cooling circuit pumps	March TE-5C-MD / Teel 1P702B
Feed circuit flow meter	Blue White 3-30 GPM
Cooling circuit flow meters	Blue White 3-30 GPM / 10-80 GPM
Thermocouples	Omega, T-type
Pressure gauges	US Gauge 0-15 psig

4.3 Data acquisition system

The permeate flux was determined manually by weighing the cooling circuit overflow. The flow rates and pressures were recorded manually. The temperatures were key variables used for establishing the existence of steady state conditions and for model predictions. They were continuously monitored by a data acquisition system. Figure 4.4 gives the schematic representation of the acquisition system. The calibration was done at the beginning following the procedure given in the owner's manual of the analog to digital converter board (DAQBOARD 200A) from Omega. The readings were periodically verified with mercury thermometers and always differed by less than 0.5°C.

4.3.1 Transducers and signal conditioner

T-type thermocouples and a high accuracy thermocouple card (DBK19) from Omega to which fourteen thermocouples could be connected were used. The connections between the thermocouples and the signal conditioner (DBK19) were done with unshielded cables.

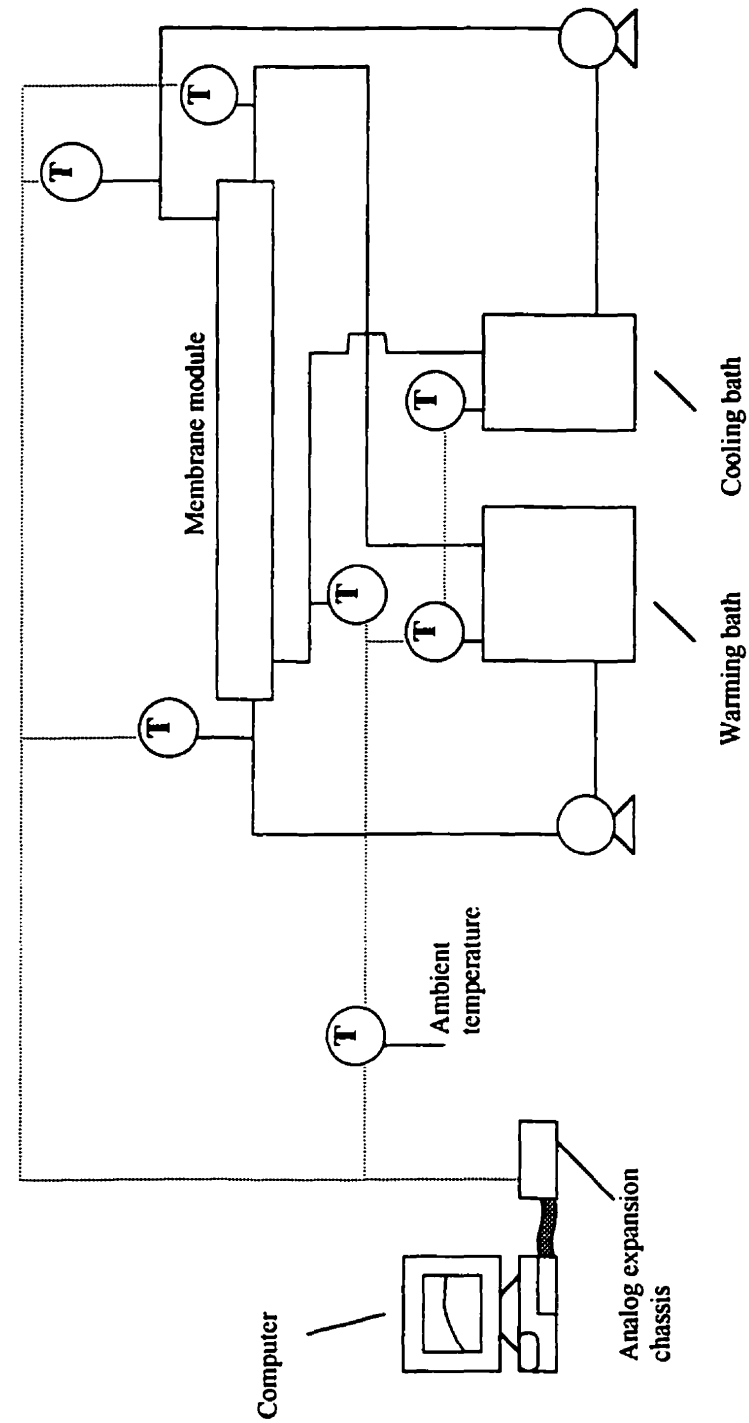

Figure 4.4 : Schematic representation of the data acquisition system

4.3.2 Analog expansion chassis

The signal conditioner cards for thermocouples (DBK19), and potentially pressure transducers (DBK11) were installed inside the Analog Expansion Chassis (DBK41 from Omega). This extension box could contain ten cards and was connected to the analog to digital board via a CA-37-x cable.

4.3.3 Analog to Digital Converter (ADC)

The ADC board (DAQBOARD 200A from OMEGA) was installed inside the computer and is configured as follows :

- Base address : 300H
- DMA and interrupt selection : DRQ7, DACK7 and IRQ15

The DAQBOARD 200A was a 16-bit ADC board to which sixteen signal conditioner cards can be connected through channels 0 to 15.

This board converted analog signals coming from the signal conditioners to digital numbers that could be used by a computer and appropriate software to store the results and to draw graphs.

4.3.4 Data acquisition software

The software used was DaqView 7.0 provided with the DAQBOARD 200A (Figure 4.5). It displays sixteen different channels corresponding to the possible signal conditioners (DBK11, DBK19...). For each used channel, the signal conditioner card must be specified and the software will then display as many sub-channels as this card could afford. For example, fifteen thermocouples could be connected to the DBK19. If this card is attributed channel 2 on the DAQBOARD 200A, then the software will display fifteen different sub-channels for the thermocouples connected to this card (2-1, 2-2, 2-3,...,2-15).

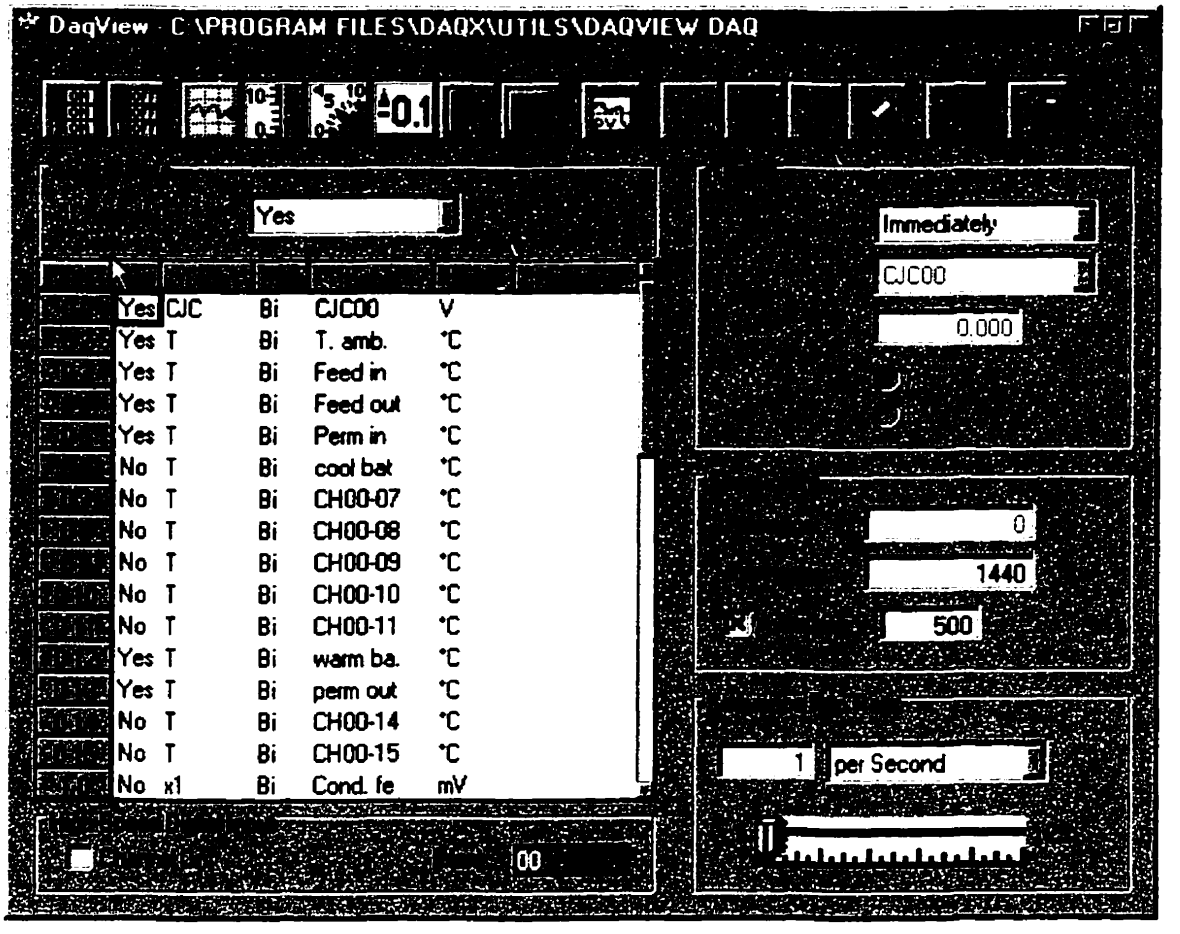

Figure 4.5 : Screen capture of the Daqview 7.0 interface

4.4 Experimental procedure

Almost all the experiments were performed with distilled water rather than saline water. It was simpler to operate and previous studies [1-3] have shown that the presence of salt (up to 5 wt.%) has little influence on the production of fresh water. A few experiments with NaCl added to distilled water were done and confirmed the earlier findings.

The parameters of the experiments were the flow rates, the temperatures and eventually the salt concentration. The flow rates on both sides of the membrane were regulated by adjusting the opening of valves V1 and V2 (Figure 4.3). The temperature of the feed and of the cooling liquid were set by adjusting the warming bath regulator and the cooling assembly. The temperature of the feed side could be controlled over a wide range (20-60°C) but the operator had little control on the temperature of the cooling liquid. Indeed, this temperature was limited by the cooling capacities of the apparatus and by coupling with the temperature of the warm side. The reference temperatures taken for the calculation were the temperatures at the entrance of the feed and cooling sides. The temperatures of the streams leaving the unit differed by less than 0.3°C from the entering values.

Levelling up and down the module at the beginning of each experiment permitted the purging of air in both circuits.

Due to the limited cooling and heating capacities, two hours were required to reach steady state. When the temperatures reached steady state, measurements of the overflow rate were taken over a period of 1 to 4 hours. The cooling circuit overflow was weighed to determine permeate flux. The overflow was then returned to the warming bath to keep its volume constant.

The saline feed was obtained by adding a given weight of sodium chloride salt to get the required concentration. To simulate sea water, a 3 to 3.5 wt.% saline water was used.

The experimental run times ranged from three to eight hours depending on the module and the experimental conditions. The experimental data are given in Appendix B.

5 Results and discussion

The membrane distillation mechanism depends upon the passage of vapour through pores. It is vital that no liquid leaks through the membrane. As will be described in section 5.1, the penetration pressure of the membrane was checked and the quality of the permeate monitored for leaks.

Fifteen experiments were conducted with the tubular membrane to ascertain that the results coincided with Prasanna [3] who used the same membrane module. This is described in section 5.2. Subsequently, eighty experiments were conducted with the hollow fibre membrane unit. A comparison of the two units for different operating conditions is presented in section 5.3. The results and semi-empirical model predictions are compared throughout that section. Section 5.4 is devoted to a comparison of the semi-empirical and theoretical models to experimental results.

5.1 Membrane wetting

Surface tension is a critical parameter in membrane distillation. It has to be high enough to balance the operating pressure. The penetration pressure, or wetting pressure, was investigated by using a 0.036 m^2 module containing three tubular membranes with the same specifications as the ones of the 1 m^2 unit. Distilled water was circulated, under pressure, inside the tubes. No water or counter pressure was applied on the other side (Figure 5.1). A pressure of 32 psi gauge (221 kPa) was applied for thirty minutes without any wetting of the membrane. The maximum pressure reached with the 1 m^2 tubular unit was of 1-2 psi gauge (7-14 kPa) far below the maximum pressure tested.

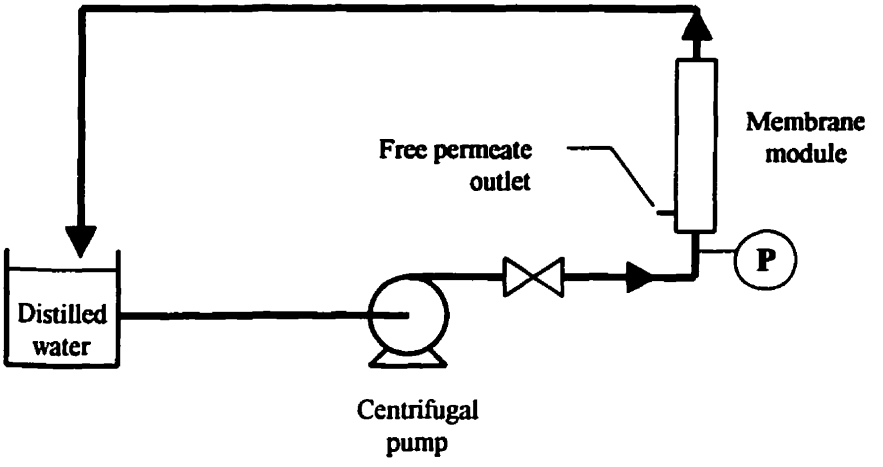

Figure 5.1 : Wetting pressure determination experiment

With the hollow fibre unit, the maximum operating pressure was of 9 psi gauge (62 kPa) on the permeate side and 6 psi gauge (41 kPa) on the feed side. This is still far below the maximum pressure tested for membrane wetting. To verify that no wetting occurred during the experiments, tests were conducted with saline water on the feed side. Had the membrane wetted, the conductivity in the cooling bath would have increased because liquid saline water would have passed through the membrane. Monitoring the cooling circuit conductivity proved that no membrane wetting occurred under the experimental conditions. Multiple experiments were done with a feed water conductivity of 45 ± 5 mS. The conductivity of the cooling water slightly decreased during the experiments as ultra-pure permeate vapour condensed in it. The cooling water conductivity never exceeded 10 μS.

No membrane wetting occurred during the experiments but only distilled water and distilled water with sodium chloride were used. Unfortunately, the presence of other compounds such as organics in less pre-treated feed would lower the surface tension which could cause membrane wetting and the failure of the process. This happened at a plant producing drinking water in the Caribs when a tanker released petroleum compounds in the sea. The plant is no longer in operation. The composition of the feed water is thus a critical parameter in desalination by membrane distillation.

5.2 *Tubular unit*

The performance of the 1 m^2 tubular unit was already investigated by Prasanna [3]. The purpose of the present experiments was to determine if the membrane characteristics were still the same in order to use the results given by Prasanna for comparison purposes.

Only distilled water was used for the investigation of the tubular unit properties. All the experiments were done at a feed flow rate of 20 L/min (Re=2000-3200, T=26-47°C) and at a cooling flow rate of also 20 L/min (Re=800-1450, T=14-39°C). At these flow rates, the permeate flux is independent of both sides' Reynolds numbers as demonstrated by Prasanna.

The temperatures were varied to get different vapour pressure differences for all the experiments. The membrane mass transfer coefficient C was found by drawing the curve $J=f(\Delta P_v)$ (Figure 5.2) and by calculating its slope.

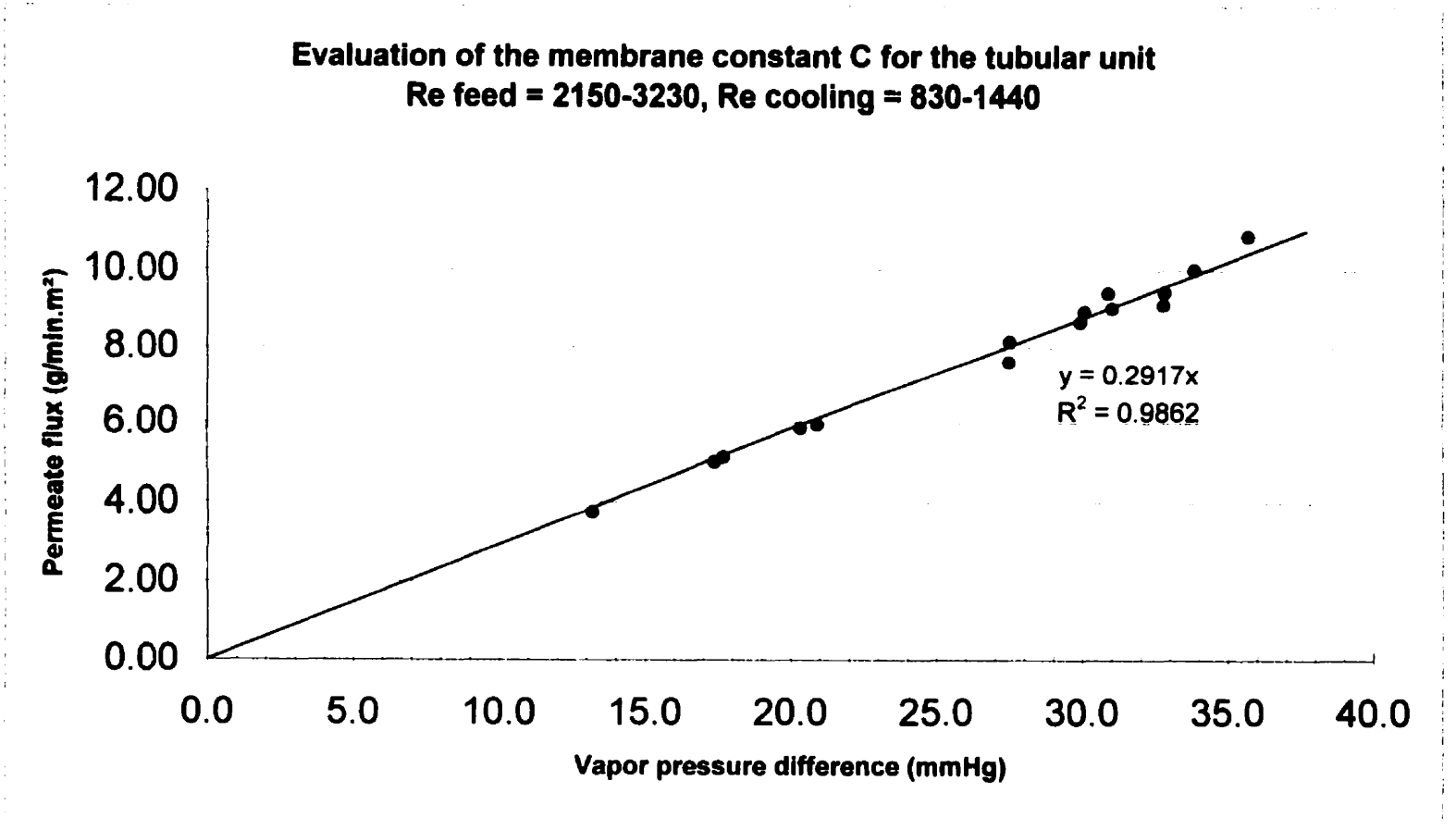

Figure 5.2 : Evaluation of the tubular membrane mass transfer coefficient

Comparing the experimental flux J to the one calculated with the model gave agreement within 5 % (Table 5.1 and Figure 5.3). The membrane constant obtained in these experiments is within $9x10^{-9}$ $kg.s^{-1}.m^{-2}.Pa^{-1}$ of that obtained by Prasanna [3]. It was concluded that since the work of Prasanna, the membrane properties have remained the same. His results could then be used for comparison purposes.

Table 5.1 : Experimental and predicted fluxes

Experiment	Experimental flux ($g.min^{-1}.m^{-2}$)	Predicted flux ($g.min^{-1}.m^{-2}$)	Difference (%)
T1	7.61	7.96	**4.4**
T2	9.42	8.96	**5.1**
T3	8.94	8.72	**2.5**
T4	8.66	8.68	**0.2**
T5-1	9.03	9.00	**0.3**
T5-2	5.12	5.01	**2.2**
T6-1	4.99	4.92	**1.4**
T6-2	8.16	7.96	**2.5**
T7	10.02	9.77	**2.6**
T8	9.12	9.46	**3.6**
T9	9.44	9.47	**0.3**
T10	5.85	5.68	**3.0**
T11	5.94	5.85	**1.5**
T12	3.75	3.60	**4.2**
T13	10.86	10.35	**4.9**

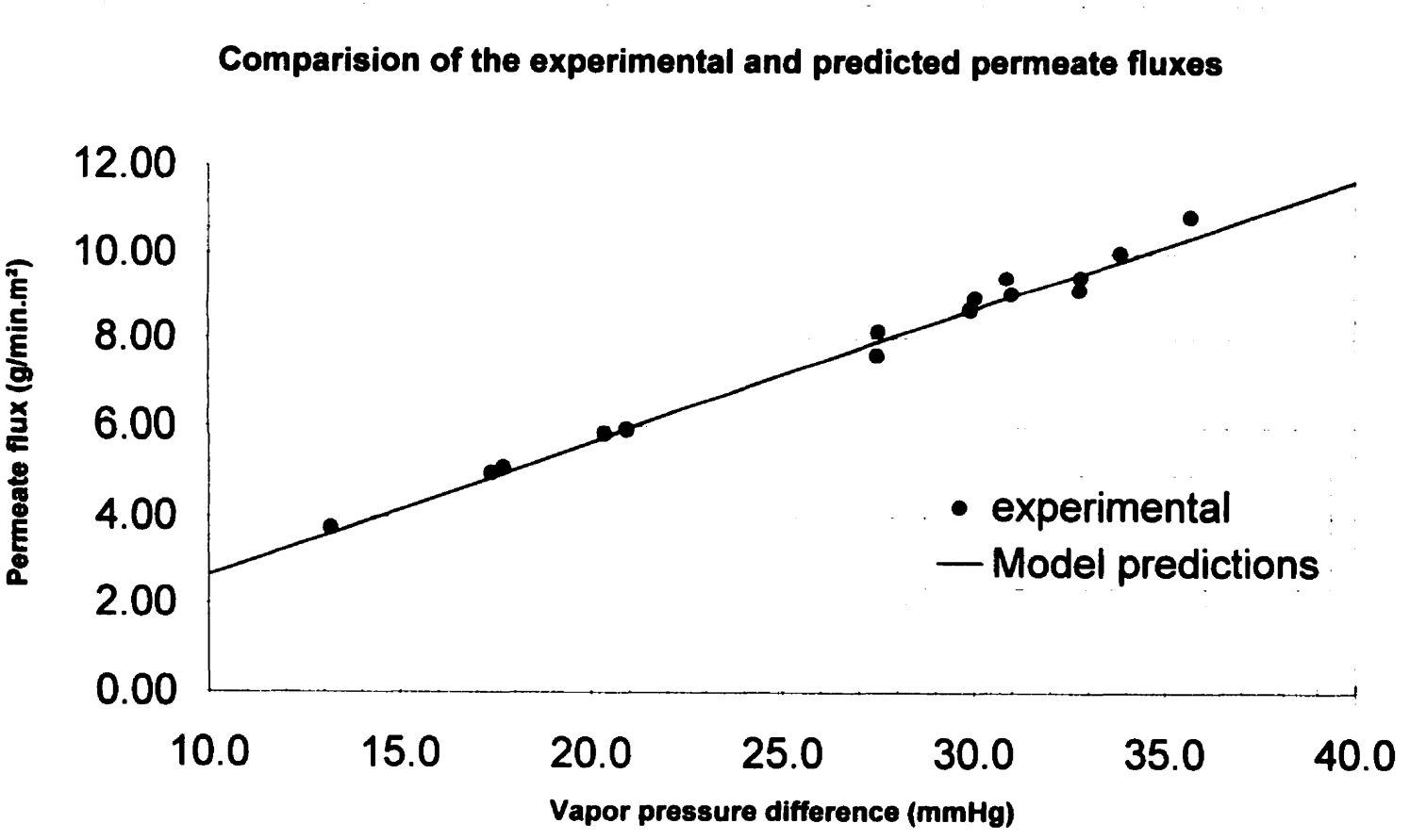

Figure 5.3 : Experimental and predicted permeate fluxes

5.3 Comparative study of the tubular and hollow fibre units

5.3.1 Effect of the temperature

As the permeate flux is a function of the vapour pressure difference ($J=C\Delta P_v$) which is itself a function of the temperature (Antoine's equation, Figure 5.4), the permeate flux is strongly affected by the feed temperature and by the temperature difference between the hot and the cold streams. In order to maximise the permeate flux, the temperature difference and the mean temperature should be as high as possible, technically and economically speaking. Unfortunately, because of the limited cooling and heating capacities of the experimental apparatus, the temperature difference did not exceed 17°C (tubular unit) and 12.5°C (hollow fibre unit).

As expected, the effects of the temperature were the same for both membrane units. The permeate flux increased with increasing feed temperature and with increasing temperature difference. The model predicts that the hollow fibre unit is the more sensitive to temperatures (Figure 5.5).

Figures 5.6 and 5.7 show in 3D the model predictions of the permeate flux for different feed temperature and temperature differences. The same trend is observed once again. The permeate flux of the hollow fibre unit was expected to exceed that of the tubular membrane unit at the same conditions.

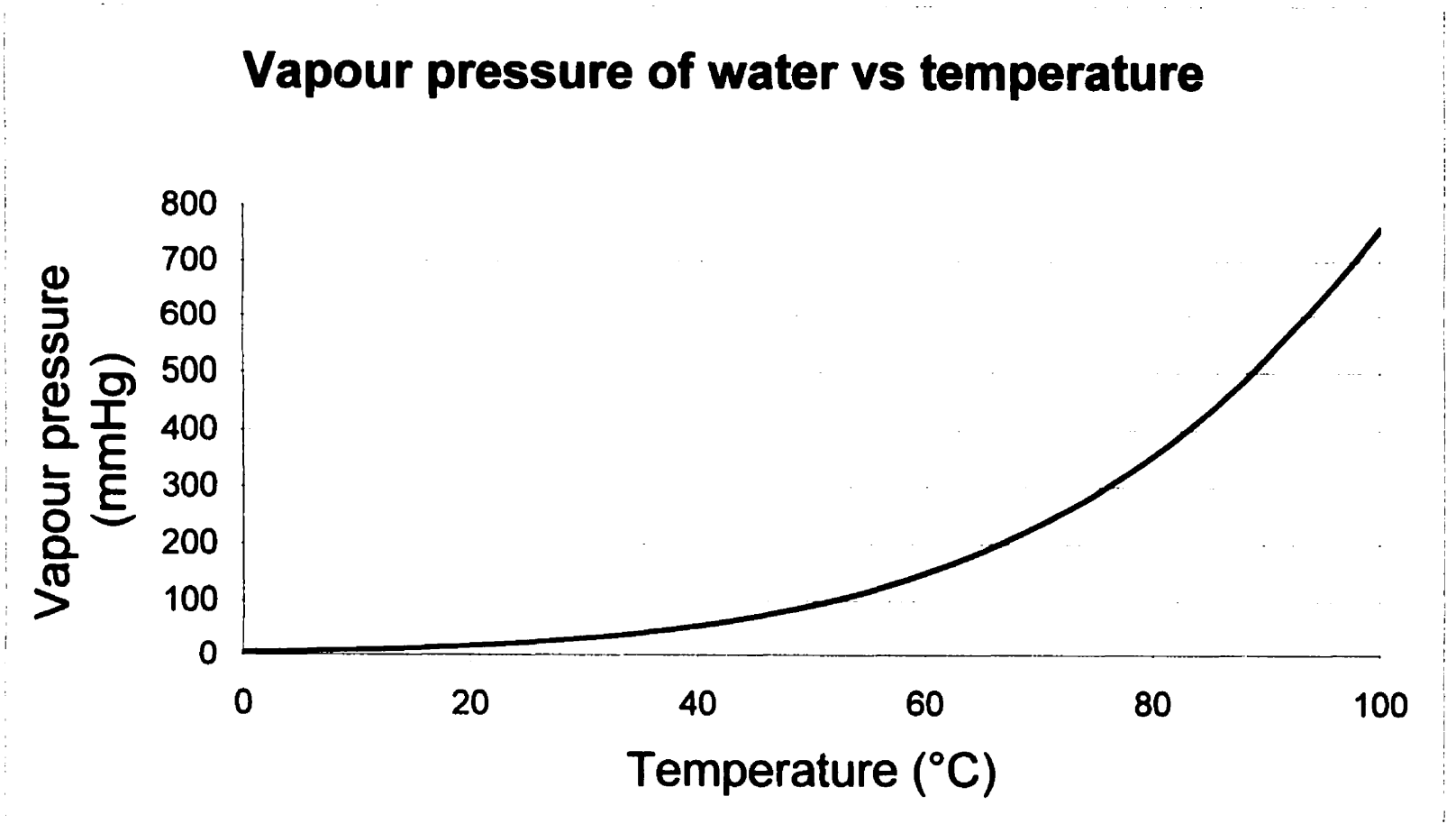

Figure 5.4 : Vapour pressure of pure water by Antoine's equation

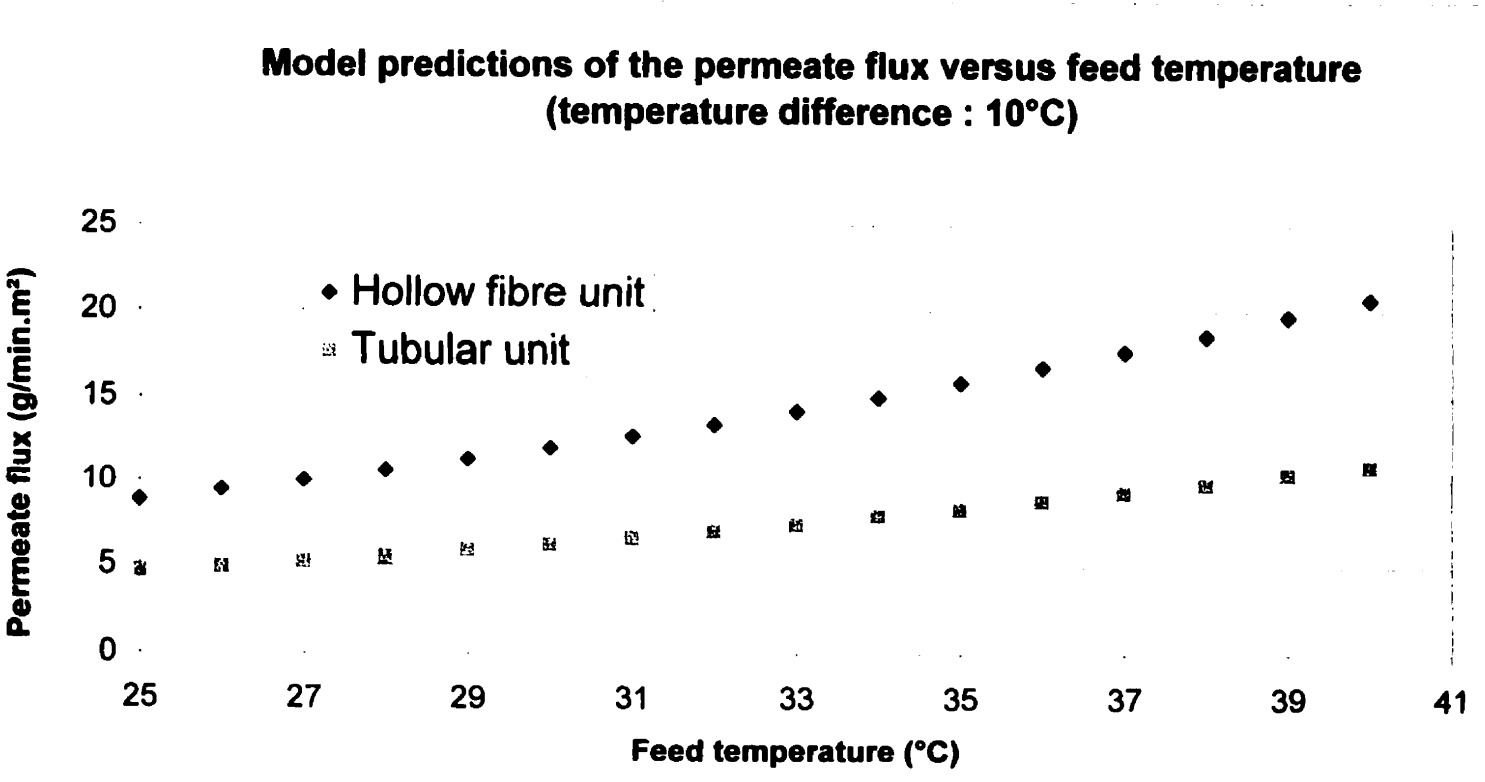

Figure 5.5 : Semi-empirical model predictions of the permeate flux

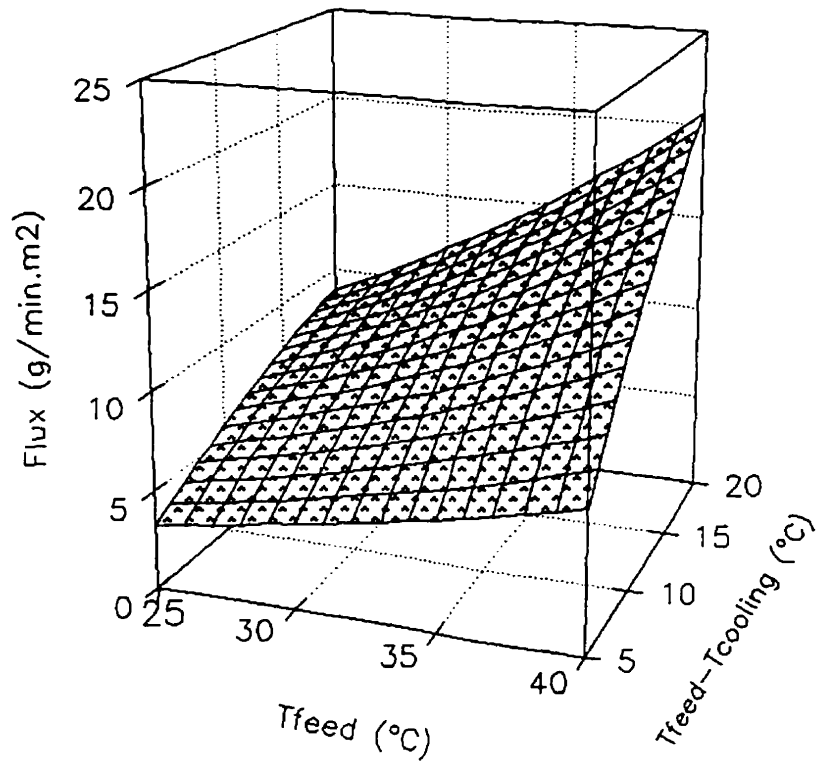

Figure 5.6 : Semi-empirical model predictions for the hollow fibre unit permeate flux

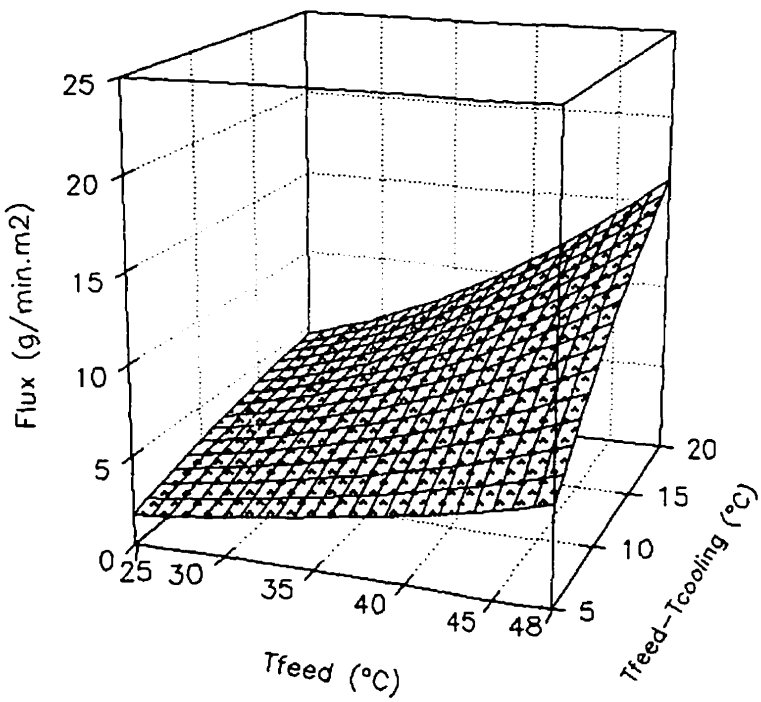

Figure 5.7 : Semi-empirical model predictions for the tubular unit permeate flux

5.3.2 Effect of the feed flow rate

Banat [1], Lacoursière [2] and Prasanna [3] have demonstrated that for the same operating conditions, increasing the feed flow rate strongly increases the permeate flux until it reaches a plateau. This phenomenon is explained by the transition between laminar and turbulent flow. In the turbulent region, temperature polarisation and concentration polarisation are minimised so the vapour pressure difference is maximised.

With the tubular unit, the plateau is reached for a feed Reynolds number around 1200, corresponding to a flow rate of 10L/min, with a saline solution (3 wt.% NaCl) [3]. During the experiments done with the hollow fibre unit (Figure 5.8) the plateau was reached a little bit sooner for a Reynolds number around 1000, corresponding to a flow rate of 30L/min (Figure 5.9). The difference is not really significant and may be explained by the use of distilled water instead of saline water. However, to achieve the same Reynolds number in the narrow hollow fibre unit as in the wide tubular unit, the feed flow rate has to be three times as high. This lead to a much higher energy consumption.

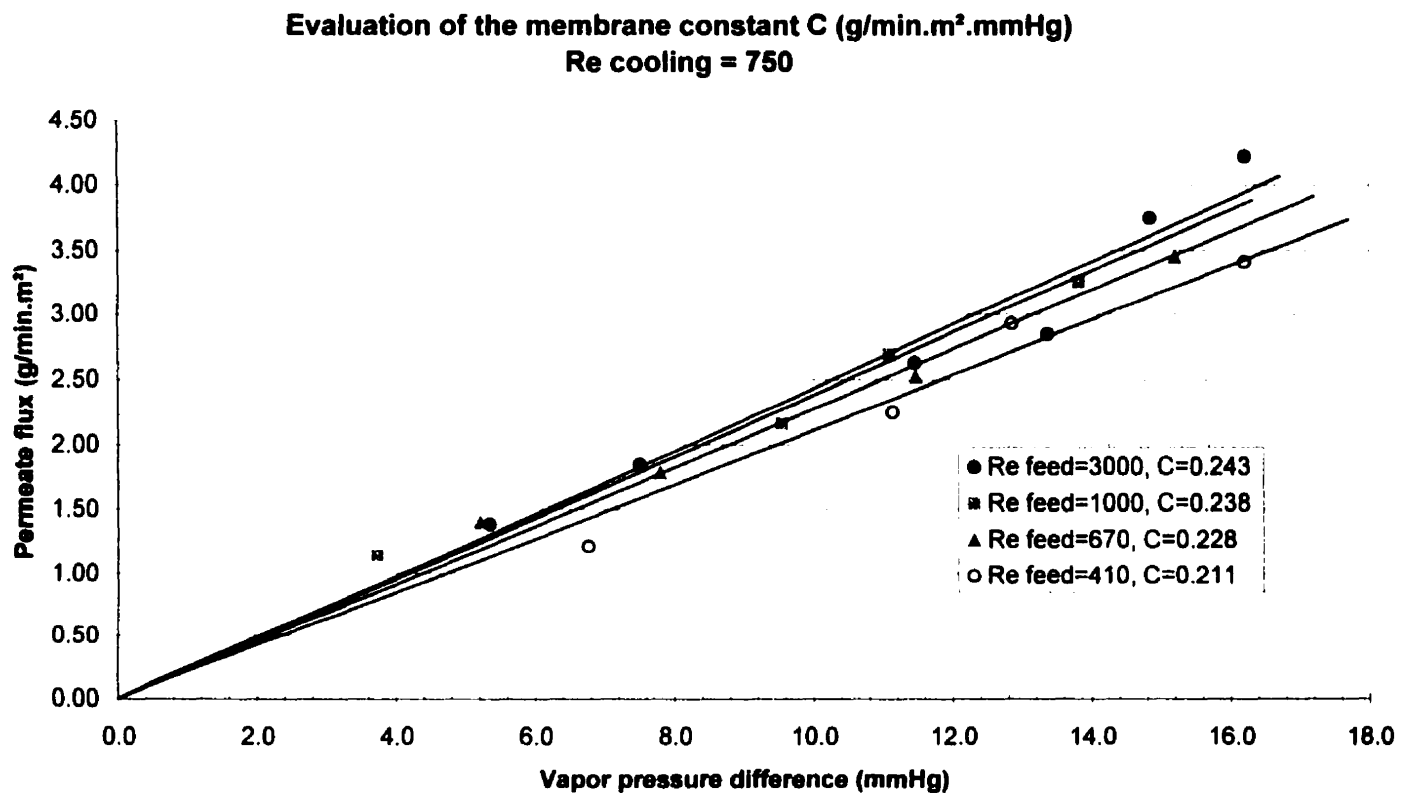

Figure 5.8 : Experimental permeate fluxes at different Reynolds numbers on the feed side

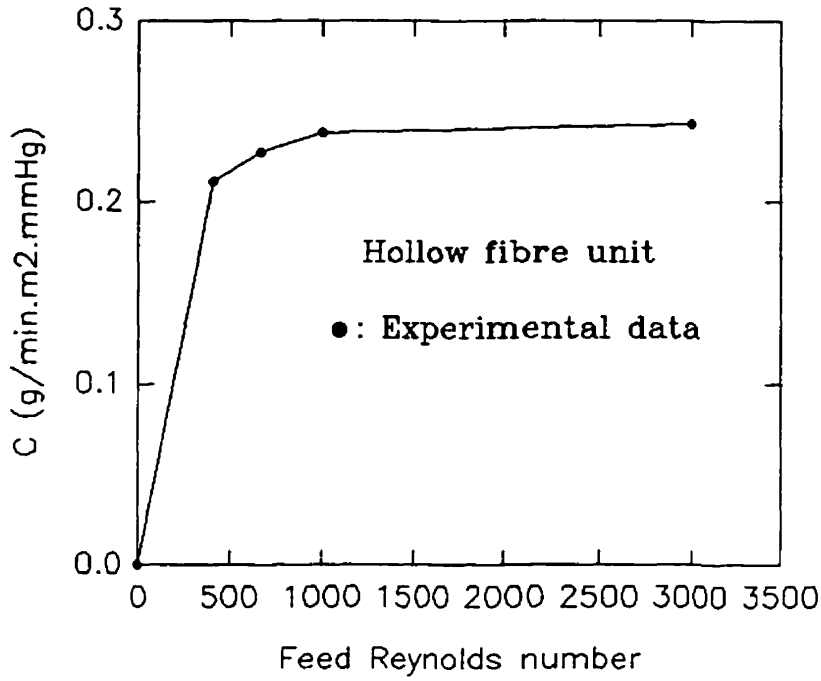

Figure 5.9 : Feed flow rate influence on the membrane mass transfer coefficient

5.3.3 Effect of the cooling flow rate

Prasanna [3] did not investigate the effect of the cooling water flow rate on the permeate flux but Lacoursière [2] did on a smaller tubular unit with only three tubes. It was demonstrated that the influence is far less significant than the one of the feed flow rate. The same trend was observed with an increase in permeate flux for an increase in cooling water flow rate until a plateau was reached at Re=1500.

However, the unit hydrodynamics have to be taken into account. The cross section temperature profile is not the same for a three or for a forty-one-tube units (Figure 5.10). The temperature of the cooling water will be much warmer in the centre of the forty-one-tube module. Increasing the flow rate will then have a greater influence by reducing the temperature of the cooling liquid in the centre of the module. The plateau will be reached when the cooling water temperature gradient will be as close as possible to zero.

The cross section temperature gradient is a serious consideration in the case of the hollow fibre unit. The fibres are extremely packed inside the module (Figure 5.11). The temperature gradient is then expected to be very high over the cross section of the unit.

This concept is supported by the experiments done with the hollow fibre unit (Figure 5.12) and by Figure 5.13 which show that the permeate flux is strongly dependent on the cooling water flow rate until it reaches a plateau at a Reynolds number of approximately 1800. The hollow fibre unit requires 95 L/min to reach the plateau versus 20 L/min for the tubular unit. Consequently, the hollow fibre unit, once again, needs more energy for pumping to reach higher permeate fluxes.

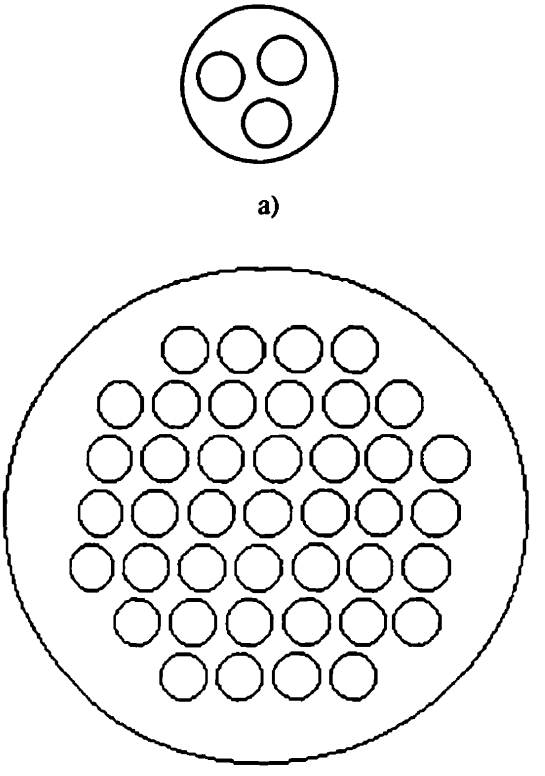

a)

b)

Figure 5.10 : Tubular unit cross sections : a) three-tubes b) forty one-tubes

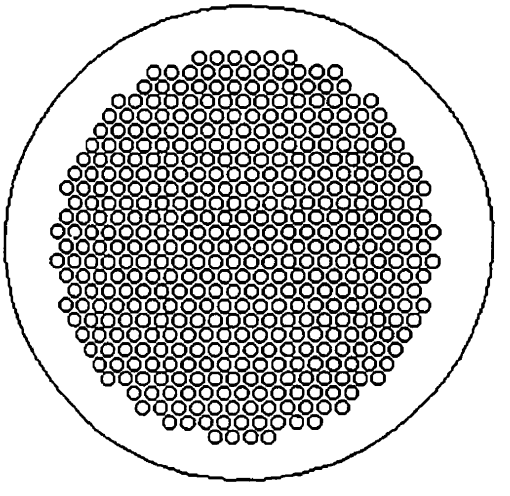

Figure 5.11 : Hollow fibre unit cross section

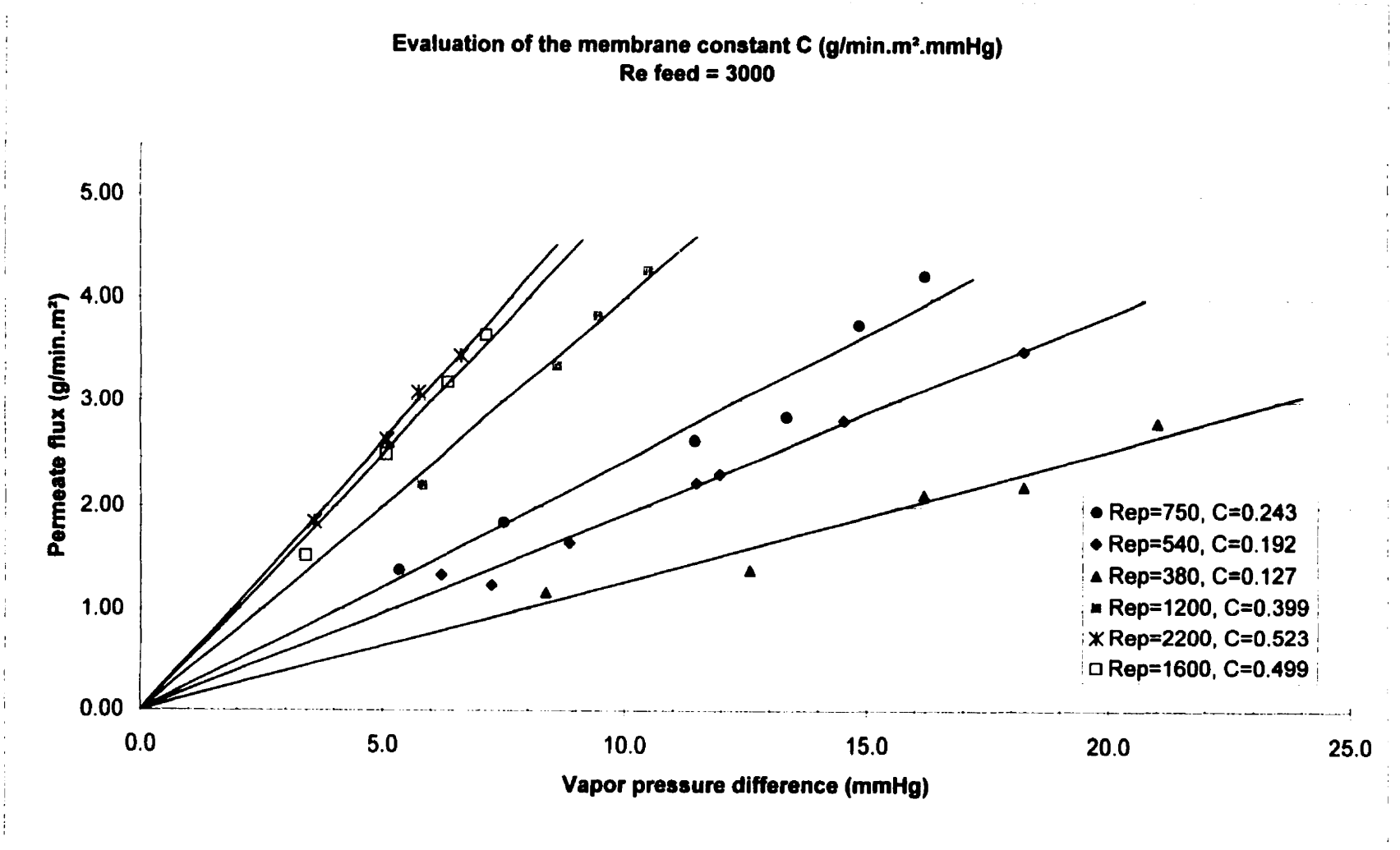

Figure 5.12 : Experimental permeate fluxes at different Reynolds numbers on the cooling side

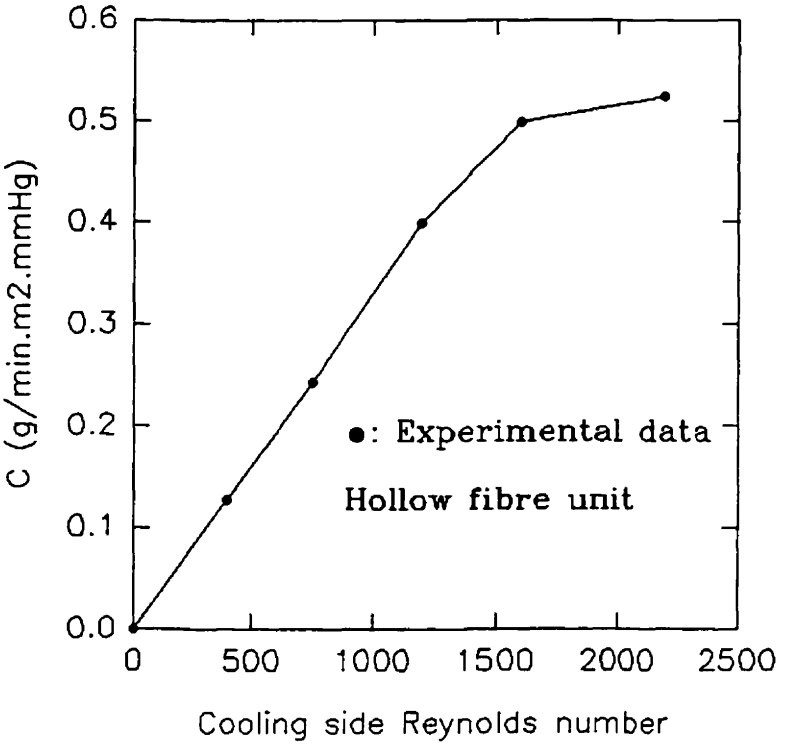

Figure 5.13 : Influence of the cooling side flow rate on the membrane mass transfer coefficient in the hollow fibre unit

5.3.4 Effect of the salt concentration

The salt concentration reduces the permeate flux by reducing the vapour pressure of water on the feed side.

Prasanna [3] did not notice a difference between a 3% NaCl solution and distilled water for the tubular unit even if theoretical calculations predict a reduction of 5% in vapour pressure.

With the hollow fibre unit, a 6% permeate flux reduction was experimentally demonstrated (for a 7.7% predicted reduction) by using a 3.4 wt.% NaCl concentration (Figure 5.14). The model predictions are, once again, good (Figure 5.15).

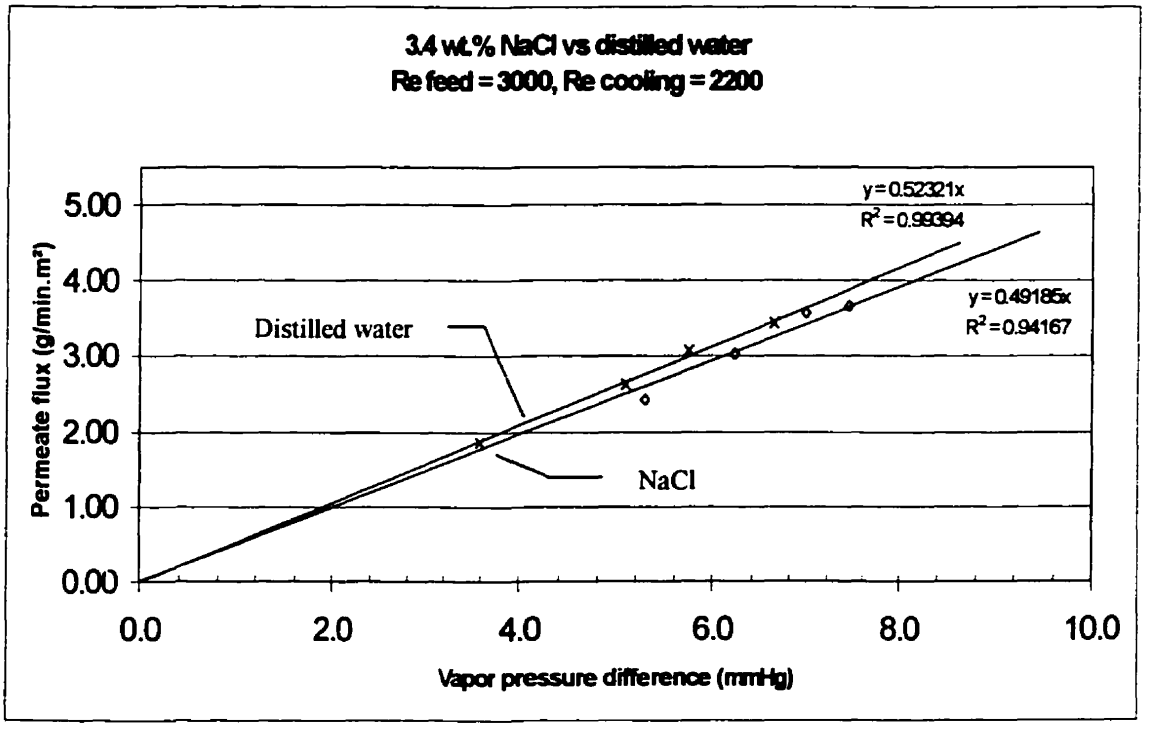

Figure 5.14 : Permeate flux with distilled water and a 3.4 wt.% NaCl feed solutions

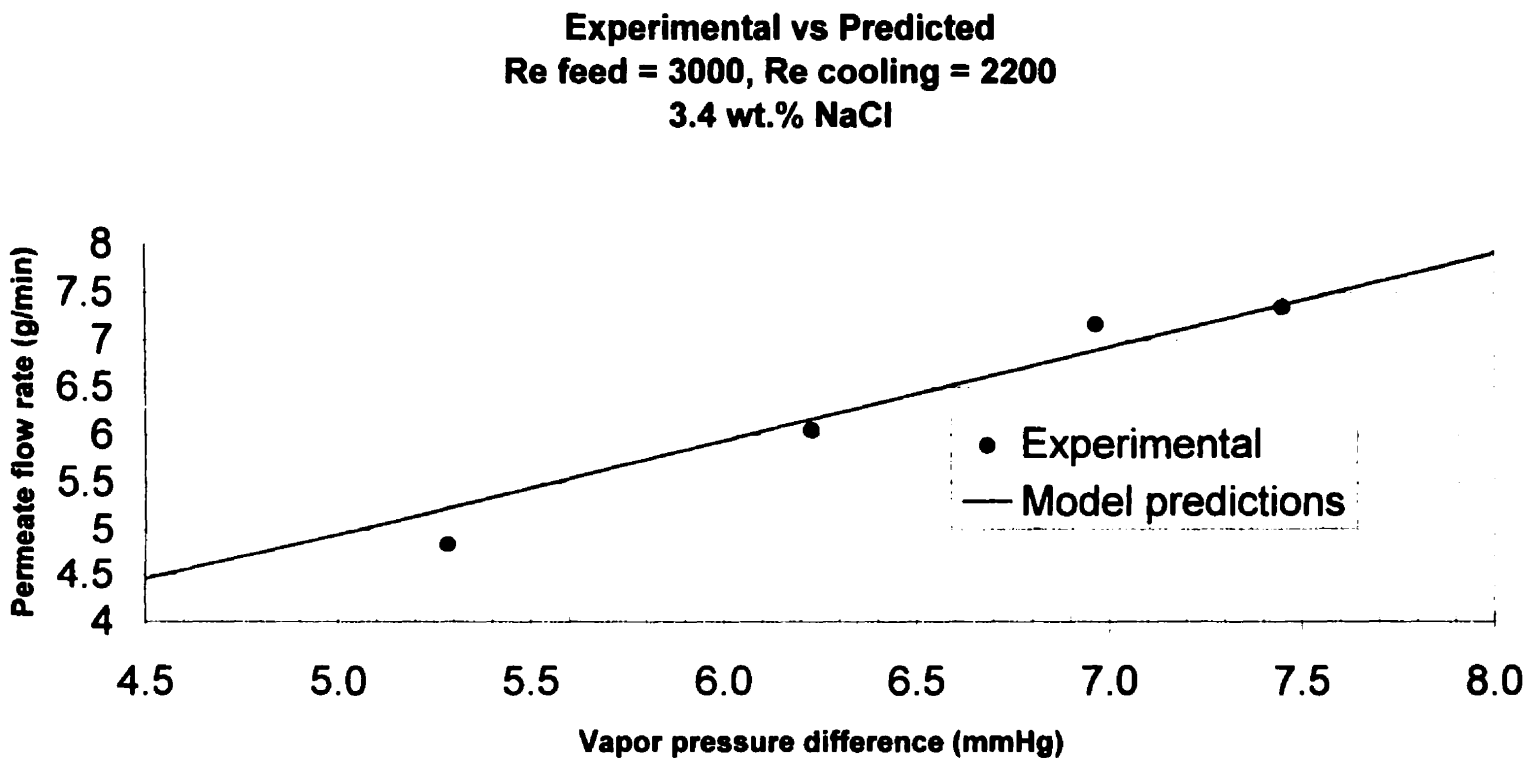

Figure 5.15 : Permeate flow rate, experimental values and model predictions for a 3.4 wt.% NaCl solution

5.3.5 Economical considerations and comparison of highest permeate fluxes achieved by the hollow fibre and tubular membrane units

As expected, the thin-walled hollow fibre unit had a higher membrane mass transfer coefficient than the thicker tubular unit. This would indicate that the permeate flux which could be achieved, for identical temperature conditions in the two units, would be greater for the hollow fibre unit than for the tubular membrane unit. Two factors prevented a conclusive experimental demonstration of this prediction. The first was the difference in hydromechanics of the two units. As mentioned in earlier sections of this chapter, the tightly packed hollow fibre unit required much higher flow rates to achieve the same Reynolds numbers as the tubular unit. Even when the same Reynolds numbers were reached, the trans-membrane temperature difference of the inner hollow fibres was less than that of the inner tubular membranes. The second difficulty was in accommodating the high heat-removal requirements of the hollow fibre unit. Although extra cooling capacity was added, it still did not allow the unit to reach its full distillation potential.

Table 5.2 summarises the operating conditions under which the highest fluxes were achieved in the two units. Although the membrane was willing, the hollow fibre unit heating, cooling and pumping peripherals were weak. It was not possible to reach comparably high trans-membrane temperatures in the hollow fibre unit as in the tubular unit. Even though the hollow fibre unit had twice as much surface area as the tubular unit, at comparable Reynolds numbers, it produced only 0.414 kg/h of fresh water compared to 0.652 kg/h produced by the tubular unit.

A preliminary economic analysis of this situation indicates that it is the operating costs which will determine the competitiveness of these units. The capital cost of the modules at this scale is comparable. The heating/cooling and pumping requirements of the hollow fibre unit exceed those of the tubular unit for comparable permeate fluxes. Peripheral equipment more powerful than bench scale would have to be involved to optimise the hollow fibre unit.

Table 5.2 : Performances and experimental conditions comparison

	Hollow fibre unit ($2m^2$)	Tubular unit ($1m^2$)
Membrane constant	$6.54*10^{-8}$ $kg.s^{-1}.m^{-2}.Pa^{-1}$	$3.65*10^{-8}$ $kg.s^{-1}.m^{-2}.Pa^{-1}$
Maximum permeate flow obtained for that constant	0.414 kg/h	0.652 kg/h
Feed side flow rate	30 L/min (Re = 1000)	10 L/min (Re = 1200)
Cooling water flow rate	95 L/min (Re = 1800)	20 L/min (Re = 1150)
Feed side temperature	33.6°C	41.2°C
Cooling water temperature	30.3°C	24.6°C
Membrane module cost	2100$ (US)	1830$ (US)

5.4 Comparison of the semi-empirical and theoretical models

The semi-empirical model fits the experimental values within 5% for the tubular membrane and within 3% for the hollow fibre membrane when using distilled water feed (Table 5.3).

Knudsen diffusion, molecular diffusion and Hagen-Poiseuille viscous flow theoretical models were also examined. The calculations were done by taking the mean temperature between the feed and the cooling water entrances. The vapour pressures were taken at these temperatures and the pressure inside the pores was assumed to be 1 atm. Due to the unavailability of tortuosity data from the manufacturer of the membranes, the tortuosity was assumed to be equal to 1.3. Details of the calculations are presented in Appendix C.

At 30°C and 1 atm, the water molecules mean free path is approximately 0.1 μm. According to the theory developed in section 3.2 and with a pore diameter of 0.2 μm, the mass transport mechanism is in the transition region between the Knudsen diffusion and the molecular diffusion. Surprisingly, the Hagen-Poiseuille viscous flow model predictions of the permeate flow rate (Table 5.3) were better than the other two although this theory is applicable to very large pore sizes compared to the mean free path of the water molecule. Its predictions are almost as good as the semi-empirical model and within 9%.

These observations mean that the Hagen-Poiseuille model is the best theoretical model to describe the combination of the transport mechanism and of the hydraulics of the modules. It does not mean that the transport mechanism follows a Hagen-Poiseuille viscous flow transport mechanism. Indeed, the temperature of the cooling water in the centre of the module was certainly not the same as at the periphery. So, the rate of the permeate flux was lowered resulting in a lower experimental flow. Only experiments with a unit containing one tube or one hollow fibre could determine which transport mechanism is happening.

Table 5.3 : Predictions of the semi-empirical and theoretical models

Run	Experimental (g/min)	Semi-empirical model (g/min) (%difference)	Knudsen flow (g/min) (% difference always greater than 300%)	Molecular diffusion flow (g/min) (% difference always greater than 100%)	Hagen-Poiseuille flow (g/min) (%difference)
67	3.70	3.78 (2.1%)	30.7	20.6	4.08 (9%)
68	5.25	5.36 (2.1%)	43.7	29.1	5.80 (9%)
69	6.17	6.11 (1.0%)	49.1	33.3	6.50 (5%)
70	6.90	7.10 (2.8%)	56.4	38.8	7.43 (7%)
T1	7.61	7.96 (4.4%)	23.5	17.7	7.93 (4%)
T2	9.42	8.96 (5.1%)	26.6	19.5	8.99 (5%)
T3	8.94	8.72 (2.5%)	25.9	19.0	8.75 (2%)
T4	8.66	8.68 (0.2%)	25.8	18.9	8.71 (1%)
T5-1	9.03	9.00 (0.3%)	26.7	19.6	9.03 (0%)
T5-2	5.12	5.01 (2.2%)	15.4	10.6	5.30 (3%)
T6-1	4.99	4.92 (1.4%)	15.2	10.4	5.21 (4%)
T6-2	8.16	7.96 (2.5%)	23.7	17.2	8.06 (1%)
T7	10.02	9.77 (2.6%)	29.6	20.4	10.14 (1%)
T8	9.12	9.46 (3.6%)	28.6	19.7	9.82 (7%)
T9	9.44	9.47 (0.3%)	28.6	19.8	9.82 (4%)
T10	5.85	5.68 (3.0%)	18.0	11.9	6.22 (6%)
T11	5.94	5.85 (1.5%)	18.5	12.2	6.41 (7%)
T12	3.75	3.60 (4.2%)	11.7	7.5	4.10 (9%)
T13	10.86	10.35 (4.9%)	31.1	21.6	10.64 (2%)

6 Conclusions and recommendations

A hollow fibre membrane module was tested and its performance was compared to that of a tubular unit. Experiments were conducted to determine the behaviour of each module for different experimental conditions (temperatures, flow rates). The following conclusions were reached :

- The range of the possible operating conditions is greatly limited by the cooling and heating capacities of the apparatus.

- The influence of the feed flow rate is almost the same for the hollow fibre and tubular membrane units. The permeate fluxes reach a plateau at turbulent flow rates.

- The influence of the cooling water flow rate is more significant in the case of the hollow fibre unit due to a strong cooling water temperature gradient perpendicular to the direction of the flow. Increasing the flow rate decreases this gradient and leads to a better permeate flux until a plateau is reached.

- The hollow fibre unit requires much higher feed and cooling water flow rates than the tubular unit to achieve turbulent flow.

- A smaller membrane thickness increases the membrane constant.

- The hollow fibre unit could give a much better permeate flux but requires higher energy input (pumping, warming and cooling).

- The hydrodynamics within a membrane distillation unit are of fundamental importance as they influence a critical variable, trans-membrane temperature.

- With the hollow fibre module, a 3.4 wt.% NaCl solution decreases the permeate flux by 6% compared to pure distilled water.

- The semi-empirical model was the best at predicting the permeate flux. Its predictions were in very good agreement with the experimental values for both the hollow fibre and tubular units (3-6.4%).

- For the theoretical models, the Hagen-Poiseuille viscous flow fitted the best the experimental results, even if the theory is not adapted to that case, because of hydrodynamics considerations.

The following recommendations may lead to improvement of the process itself and its evaluation :

- More powerful heating and cooling apparatus should be used to evaluate the modules' capacities on a wider range of temperatures and temperature differences.

- An economic study of heating, cooling and pumping requirements should be done to determine whether or not the greater permeate flux which could be achieved by the hollow fibre unit compensates for the higher energy consumption.

- A spiral-wound configuration should be tested. Such membranes are thinner and may advantageously combine the lower flow rates of the tubular membranes with the higher membrane area and permeate fluxes of the hollow fibres to produce profitable permeate fluxes.

7 References

1. BANAT, F., *Membrane Distillation for Desalination and Removal of Volatile Organic Compounds from Water*, Ph.D. thesis, McGill University, Quebec, Canada, 1994.

2. LACOURSIÈRE, S., *Water Purification by Membrane Distillation*, M.Eng. thesis, McGill University, Quebec, Canada, 1994.

3. PRASANNA, P.R.M., *A Study and Scale-up of Desalination via Membrane Distillation*, M.Eng. thesis, McGill University, Quebec, Canada, 1998.

4. FINDLEY, M.E., *Vaporization Through Porous Membranes*, Ind. Eng. Chem. Process Des. Dev., 6, 226-230, 1967.

5. LAWSON, K.W., DOUGLAS, R.L., *Membrane Distillation*, Journal of Membrane Science, 124, 1-25, 1997.

6. BRYK, M.T., NIGMATULLIN, R.R., *Membrane Distillation*, Russian Chemicals Reviews, 63 (12), 1047-1062, 1994.

7. LAGANÁ, F., BARBIERI, G., DRIOLI, E., *Direct Contact Membrane Distillation : Modelling and Concentration Experiments*, 166, 1-11, 2000.

8. TOMASZEWSKA, M., *Concentration and Purification of Fluosilicic Acid by Membrane Distillation*, Ind. Eng. Chem. Res., 39, 3038-3041, 2000.

9. ZAKRZEWSKA-TRZNADEL, G., HARASIMOWICZ, M., CHMIELEWSKI, A.G., *Concentration of Radioactive Components in Liquid Low-Level Radioactive Waste by Membrane Distillation*, Journal of Membrane Science, 163, 257-264, 1999.

10. GREKOV, K.B., SENATOROV, V.E., *Processing of Liquid Photographic Waste by Contact Membrane Distillation*, Russian Journal of Applied Chemistry, 72, 1577-1580, 1999.

11. RINCÓN, C., ORTIZ DE ZÁRATE, J.M., MENGUAL, J.I., *Separation of Water and Glycols by Direct Contact Membrane Distillation*, Journal of Membrane Science, 158, 155-165, 1999.

12. GRYTA, M., KARAKULSKI, K., *The Application of Membrane Distillation for the Concentration of Oil-Water Emulsions*, 121, 23-29, 1999.

13. COUFFIN, N., CABASSUD, C., LAHOUSSINE-TURCAUD, V., *A New Process to Remove Halogenated VOCs for Drinking Water Production : Vacuum Membrane Distillation*, Desalination, 117, 233-245, 1998.

14. BANAT, F.A., SIMANDL, J., *Membrane Distillation for Propanone Removal from Aqueous Streams*, Journal of Chemical Technology and Biotechnology, 75, 168-178, 2000.

15. BANAT, F.A., SIMANDL, J., *Membrane Distillation for Dilute Ethanol Separation from Aqueous Streams*, Journal of Membrane Science, 163, 333-348, 1999.

16. BANAT, F.A., SIMANDL, J., *Removal of Benzene Traces from Contaminated Water by Vacuum Membrane Distillation*, Chemical Engineering Science, 51(8), 1257-1265, 1996.

17. BURGOYNE, A., VAHDATI, M.M., *Permeate Flux Modeling of Membrane Distillation*, Filtration and Separation, 49, January-February 1999.

18. MARTINEZ-DIEZ, L., VASQUEZ-GONSALEZ, M.I., *Effects of Polarization on Mass Transport Through Hydrophobic Porous Membranes*, Ind. Eng. Chem. Res., 37, 4128-4135, 1998.

19. PENA, L., GODINO, M.P., MENGUAL, J.I., *A Method to Evaluate the Net Membrane Distillation Coefficient*, Journal of Membrane Science, 143, 219-233, 1998.

20. GRYTA, M., TOMASZEWSKA, M., *Heat Transport in Membrane Distillation Process*, Journal of Membrane Science, 144, 211-222, 1998.

21. MARTINEZ-DIEZ, L., VASQUEZ-GONSALEZ, M.I., *Temperature and Concentration Polarization in Membrane Distillation of Aqueous Salt Solutions*, Journal of Membrane Science, 156, 265-273, 1999.

22. BURGOYNE, A., VAHDATI, M.M., *Direct Contact Membrane Distillation*, Separation Science and Technology, 35(8), 1257-1284, 2000.

23. PERRY, R.H., GREEN, D.W., MALONEY, J.O., *Perry's Chemical Engineer's Handbook*, 7th edition, McGraw-Hill, New-York, NY, pp.2-320-2-321,2-370, 1997.

24. SCHOFIELD, R.W., FANE, A.G., FELL, C.J.D., *Heat and Mass Transfer in Membrane Distillation*, Journal of Membrane Science, 33, 299-313, 1987.

25. SCHOFIELD, R.W., FANE, A.G., FELL, C.J.D., *Gas and Vapour Transport Through Microporous Membranes. I. Knudsen-Poiseuille Transition*, Journal of Membrane Science, 53, 159-171, 1990.

26. SCHOFIELD, R.W., FANE, A.G., FELL, C.J.D., *Gas and Vapour Transport Through Microporous Membranes. II. Membrane Distillation*, Journal of Membrane Science, 53, 173-185, 1990.

27. BIRD, R. B., STEWART, W. E., LIGHTFOOT, E. N., *Transport Phenomena*, John Wiley & Sons, 1960.

28. BENNETT, C.O., MEYERS, J.E., *Momemtum, Heat and Mass Transfer*, McGraw-Hill, New-York, NY, p.802, 1982.

29. BRETSZNAJDER, S., *Predictions of Transport and Other Physical Properties of Fluids*, Pergamon Press, Oxford, UK, pp.189-239, pp.289-328, 1971.

30. COULSON, J.M., RICHARDSON, J.F., *Chemical Engineering: Volume 1-Fluid Flow, Heat Transfer, and Mass Transfer*, Pergamon Press, Oxford, UK, pp.312-441.

31. GEANKOPLIS, C., *Transport Processes and Unit Operations*, Prentice-Hall, Englewood Cliffs,, NJ, pp.426-488, 1993.

Appendix A

Flux prediction program

```
'FLUX.xls
'
'THIS PROGRAM CALCULATES THE FLUX OF A MEMBRANE DISTILLATION
'UNIT
'
'THE CODE IS BASED ON THE ONE WRITTEN BY PRASANNA [3] IN FORTRAN.
'IT HAS BEEN ADAPTED AND WRITTEN IN VISUAL BASIC BY
'LUDOVIC PLASSE
'NOVEMBER 2000

Option Explicit

    Dim km, kg, porosity, delta, id, od, pore, length As Double
    Dim Clarge, C, Pfm, Ppm, Evap, Cfm As Double
    Dim TfC, QFlm, TpC, QPlm, TfK, wtf, wtfm, rhof, conc, mufp, mufm, muf, kf20, kf
    As Double
    Dim TpK, mupp, mup, rhop, Tfilm, mufip, mufi, rhofilm, massf, massp As Double
    Dim QFm3, QPm3, hc, vf, Ref, Prf, Nuf, hf, vp, parea, dhyd, Rep, Prp, Nup As
    Double
    Dim hp, sid, Cpf, kp, Cpp, TfilmK, mufipv, rhofilmv, diff, Sc, Ks, area As Double
    Dim Jtot, Error, Tol, guess, Tp, Tpm, Tf, Tfm, Jseg, Qv, Qc, Q, Jfibre, J As Double
    Dim Gain, hv, wfm, TpI, TfI, hp2 As Double
    Dim Qheat As Double
    Dim segment, num, I, dT As Integer
```

```
Sub calcul()

'UNIVERSAL MEMBRANE PROPERTIES
'UNITS: kg,km[W/mK];

   km = 0.14      ' Membrane Thermal Conductivity @ 50øC
   kg = 0.0235    ' Thermal Conductivity Air/Water @ 50øC
   porosity = 0.75 ' Porosity of the Membranes


If UserForm1.OptionButton_1m2.Value = True Then
'1 m^2 TUBULAR MEMBRANE PROPERTIES
'UNITS: Clarge[kg/s m2 Pa]; delta,id,od,pore,length,mid [m];

   Clarge = 0.000000046585
   delta = 0.0015   ' Membrane Thickness- Vapour path length
   id = 0.0055      ' Membrane Inner Diameter
   od = 0.0085      ' Membrane Outer Diameter
   pore = 0.0000002  ' Pore Size
   length = 1.27    ' Membrane Length
   num = 41         ' Number of Tubes
   segment = 91     ' Number of Segments
   sid = 0.09       ' Shell inner diameter-estimate
   C = Clarge

ElseIf UserForm1.OptionButton_2m2.Value = True Then
'2 m^2 HOLLOW FIBERS MEMBRANE PROPERTIES
'UNITS: Clarge[kg/s m2 Pa]; delta,id,od,pore,length,mid [m];

   Clarge = 0.000000065407
   delta = 0.0004   ' Membrane Thickness- Vapour path length
```

```
    id = 0.0018      ' Membrane Inner Diameter
    od = 0.0026      ' Membrane Outer Diameter
    pore = 0.0000002 ' Pore Size
    length = 0.875   ' Membrane Length
    num = 450        ' Number of Tubes
    segment = 91     ' Number of Segments
    sid = 0.085      ' Shell inner diameter-estimate
    C = Clarge
End If

'FEED CONDITIONS INPUT


  If IsNumeric(UserForm1.TextBox_Tfeed.Value) = False Then
    UserForm1.TextBox_Tfeed.Value = ""
    UserForm1.TextBox_Tfeed.SetFocus
    Exit Sub
  End If


  If IsNumeric(UserForm1.TextBox_Flowfeed.Value) = False Then
    UserForm1.TextBox_Flowfeed.Value = ""
    UserForm1.TextBox_Flowfeed.SetFocus
    Exit Sub
  End If

  If IsNumeric(UserForm1.TextBox_Saltconcentration.Value) = False Then
    UserForm1.TextBox_Saltconcentration.Value = ""
    UserForm1.TextBox_Saltconcentration.SetFocus
    Exit Sub
  End If
```

```
TfC = CDbl(UserForm1.TextBox_Tfeed.Value)
QFlm = CDbl(UserForm1.TextBox_Flowfeed.Value)
wtfm = CDbl(UserForm1.TextBox_Saltconcentration.Value) '[g/L]
wtf = wtfm / 1000 '[kg/L] or [kg/kg]

'COOLING WATER CONDITIONS INPUT

If IsNumeric(UserForm1.TextBox_Tcooling.Value) = False Then
  UserForm1.TextBox_Tcooling.Value = ""
  UserForm1.TextBox_Tcooling.SetFocus
  Exit Sub
End If


If IsNumeric(UserForm1.TextBox_Flowcooling.Value) = False Then
  UserForm1.TextBox_Flowcooling.Value = ""
  UserForm1.TextBox_Flowcooling.SetFocus
  Exit Sub
End If

TpC = CDbl(UserForm1.TextBox_Tcooling.Value)
QPlm = CDbl(UserForm1.TextBox_Flowcooling.Value)
```

```
'FEED WATER PROPERTIES EVALUATION
'UNITS: TfK[K],mufp[Poise],mufm[Pa*s],muf[Pa*s],rhof[kg/m^3]
'conc[mol NaCl/L solution],kf20,kf[W/mK],Cpf[J/(kg K)]
'mufp calculates the pure water viscosity.  mufp is from [28], p 802. Then mufm converts
'this viscosity. The final viscosity is computed using an equation from [29], p228.

  TfK = TfC + 273.15

  If wtfm = 0 Then
    conc = 0
    rhof = 0.0000000023076 * (TfC ^ 5) - 0.00000068283 * (TfC ^ 4) + 0.00008895 *
    (TfC ^ 3) - 0.0093 * (TfC ^ 2) + 0.08 * TfC + 999.8011
    mufp = 1 / (2.1482 * ((TfC - 8.435) + ((8078.4 + (TfC - 8.435) ^ 2) ^ 0.5)) - 120)
    muf = mufp * 0.1        '[28], p802
    kf = -0.4732943 + 0.00579948887 * TfK - 0.00000725519 * (TfK ^ 2)
    Cpf = (45.359165 - 0.416094 * TfK + 0.00220052 * (TfK ^ 2) -
    0.000004380770923 * (TfK ^ 3) + 3.275994572E-09 * (TfK ^ 4)) * 1000 'Heat
    Capacity of Liquid Water

  Else
    rhof = (0.7227 * (wtf) - 0.00033 * TfC + 1.003198) * 1000 ' NaCl Density
    conc = wtf * (1 / 58.5) * rhof
    mufp = 1 / (2.1482 * ((TfC - 8.435) + ((8078.4 + (TfC - 8.435) ^ 2) ^ 0.5)) - 120)
    mufm = mufp * 0. 1        '[28], p802
    muf=mufm * (1 + 0.0062 * (conc ^ 0.5) + 0.0793 * conc + 0.008 * (conc ^ 2)) ' [29]
    kf20 = (0.515 - 0.0047 * conc) * 1000 * 4.1868 / 3600        ' [29], page 323
    kf = kf20 * ((-1 / 103125) * (TpC ^ 2) + (4877 / 1650000) * TpC + (155957 /
   165000))
    Cpf = (4.170528 - 5.55245 * wtf + 9.19117 * (wtf ^ 2) + 0.0001737824 * TfC +
    0.00001335187 * (TfC ^ 2)) * 1000
  End If
```

```
'PERMEATE WATER PROPERTIES EVALUATION
'UNITS: TpK[K],mupp[Poise],mup[Pa*s],rhop[kg/m^3], kp[W/(m*K)]
'Cpp[J/(kg*K)]

   TpK = TpC + 273.15
   rhop = 0.0000000023076 * (TpC ^ 5) - 0.00000068283 * (TpC ^ 4) + 0.00008895 *
   (TpC ^ 3) - 0.0093 * (TpC ^ 2) + 0.08 * TpC + 999.8011 ' Matlab Curve Fitting
   mupp = 1 / (2.1482 * ((TpC - 8.435) + ((8078.4 + (TpC - 8.435) ^ 2) ^ 0.5)) - 120)
   mup = mupp * 0.1            ' [28], p.802
   kp = -0.4732943 + 0.00579948887 * TpK - 0.00000725519 * (TpK ^ 2)
   Cpp = (45.359165 - 0.416094 * TpK + 0.00220052 * (TpK ^ 2) - 0.000004380770923
* (TpK ^ 3) + 3.275994572E-09 * (TpK ^ 4)) * 1000 'Heat Capacity of Liquid Water


'FILM TEMPERATURE PROPERTIES
'UNITS: Tfilm[øC],TfilmK[K],mufip[Poise],mufi[Pa*s],rhofilm[kg/m^3]
'      mufipv[Pa*s]

   Tfilm = (TfC + TpC) / 2
   TfilmK = Tfilm + 273.15
   mufip = 1 / (2.1482 * ((Tfilm - 8.435) + ((8078.4 + (Tfilm - 8.435) ^ 2) ^ 0.5)) - 120)
   mufi = mufip * 0.1  ' [28], p 802
   rhofilm = 0.0000000023076 * (Tfilm ^ 5) - 0.00000068283 * (Tfilm ^ 4) +
   0.00008895 * (Tfilm ^ 3) - 0.0093 * (Tfilm ^ 2) + 0.08 * (Tfilm) + 999.8011
   mufipv = -0.000002909707 + 0.00000004000022 * TfilmK ' Viscosity of Water(Vap.)
   rhofilmv = 0.004971907 + 0.00024676 * Tfilm + 0.00001746339 * (Tfilm ^ 2) -
   4.06779996E-08 * (Tfilm ^ 3) + 0.000000004339217 * (Tfilm ^ 4) ' **Vapour**
```

```
'MASS AND VOLUMETRIC FLOW RATES

  massf = QFlm * rhof / 1000 / 60
  massp = QPlm * rhop / 1000 / 60
  QFm3 = QFlm * (1 / 60) * (1 / 1000)
  QPm3 = QPlm * (1 / 60) * (1 / 1000)


'ESTIMATION OF hc, CONDUCTIVE HEAT TRANSFER COEFFICIENT
'UNITS: hc [W/(m^2*K)]

  hc = ((porosity * kg) + ((1 - porosity) * km)) / delta


'ESTIMATION OF hf, CONVECTIVE HEAT TRANSFER COEFFICIENT
'UNITS: hf [W/(m^2*K)]

  vf = QFm3 / (num * 3.141592654 * (id ^ 2) / 4) 'Velocity of Feed
  Ref = Re(rhof, vf, id, muf)       'Reynolds Number of Feed
  Prf = Pr(Cpf, muf, kf)            'Prandtl Number of Feed
  Nuf = Nusselt(Ref, Prf)
  'Nuf=0.023*(Ref^0.8)*(Prf^0.3)    ' Nusselt Number-Dittus-Boelter
  hf = (Nuf * kf) / id              ' Heat Transfer Coeffecient


'ESTIMATION OF hp, CONVECTION HEAT TRANSFER COEFFICIENT
'UNITS:

  dhyd = (sid ^ 2 - num * (od ^ 2)) / (sid + num * od) ' Hydraulic Diameter
  parea = 3.141592654 * 0.25 * (sid ^ 2 - num * (od ^ 2)) ' Area for permeate flow
  vp = QPm3 / parea                 ' Velocity of Permeate
```

```
Rep = Re(rhop, vp, dhyd, mup)     ' Reynolds Number of Permeate
Prp = Pr(Cpp, mup, kp)            ' Prandtl Number of Permeate
Nup = Nusselt(Rep, Prp)
hp2 = (Nup * kp) / dhyd           ' Heat Transfer Coeffecient
'Nup=0.023*(Rep^0.8)*(Prp^0.4)    ' Nusselt Number-Dittus-Boelter
hp = 4280 * (0.00488 * TpK - 1) * (vp ^ 0.8) / (dhyd ^ 0.2) 'Correlation-[30],p369


'ESTIMATION OF Ks- SOLUTE MASS TRANSFER COEFFICIENT
'UNITS: diff [m^2/s]

diff = 0.000025                          'Diffusivity of Water in Air
Sc = (mufipv / (rhofilmv * diff))        'Schmidt Number
Ks = 0.023 * (Ref ^ 0.83) * (Sc ^ 0.33) * diff / id      '[31], p442,3rd. ed.


'LOOP WHICH CALCULATED THE FLUX AS A FUNCTION OF TEMPERATURE
'ALONG THE FIBRE LENGTH

area = 3.141592654 * id * length / segment ' Inside area/segment
Jtot = 0
Error = 1
Tol = 0.005
guess = TpC + 0.2

Do

  Tp = guess
  Tpm = Tp
  Tf = TfC
  Tfm = Tf
```

```
    wfm = wtf * 100 'Weight Percentage neglecting weight increase
                    'of solution when adding salt

    For I = 1 To segment
      J = flux(C, Tfm, Tpm, hf, hc, hp, hv, rhof, Ks)
      Jseg = J * area      ' Volumetric Flux per segment
      Jtot = Jtot + Jseg   ' Cumulative Volumetric Flux
      Qv = hv * (Tfm - Tpm)
      Qc = hc * (Tfm - Tpm)
      Q = area * (Qv + Qc)
      TfI = (Tf + 273.15) - (Q / (Cpf * massf))
      Tf = TfI - 273.15
      TpI = (Tp + 273.15) - (Q / (Cpp * massp))
      Tp = TpI - 273.15
    Next

    Jfibre = ((Jtot * 3600) / (3.141592654 * id * length))
    Gain = 0.1
    Error = TpC - Tp

    If Abs(Error) >= Tol Then
      guess = guess + (Gain * Error)
      Jtot = 0
    End If

  Loop While Abs(Error) >= Tol

'Calculation of the total heat transfer
If UserForm1.OptionButton_1m2.Value = True Then
'1 m^2 TUBULAR MEMBRANE PROPERTIES
Qheat = hf * (TfC - Tfm) + hc * (Tfm - Tpm) + hv * (Tfm - Tpm) + hp * (Tpm - TpC)
```

```
ElseIf UserForm1.OptionButton_2m2.Value = True Then
'2 m^2 HOLLOW FIBERS MEMBRANE PROPERTIES
Qheat = 2 * (hf * (TfC - Tfm) + hc * (Tfm - Tpm) + hv * (Tfm - Tpm) + hp * (Tpm -
TpC))

End If

UserForm1.Label_Flowrate = Jtot * num * 60 * 1000
UserForm1.Label_Reynolds_feed = Int(Ref)
UserForm1.Label_Reynolds_perm = Int(Rep)
UserForm1.Label_Heattransfer = Int(Qheat)

End Sub
```

```
Function flux(C_membrane, Tfeedm, Tpermeatm, hconvective, hconductive,
hconvection, hvapo, rhofeed, Ksolute)

Dim Jprev As Double

Pfm = VPf(Tfeedm, wfm)
Ppm = VPp(Tpermeatm)
flux = C_membrane * (Pfm - Ppm) * (101325 / 760)
Jprev = 20

Do While Abs(flux - Jprev) >= 0.0000000005 And flux > 0
   Evap = Hvap(Tfeedm) * 1000
   hvapo = (flux * Evap) / (Tfeedm - Tpermeatm)
```

```
   Tfeedm = Tf - ((Tf - Tp) * (1 / hconvective) / ((1 / (hvapo + hconductive)) + (1 /
hconvective) + (1 / hconvection)))
   Tpermeatm = Tp + ((Tf - Tp) * (1 / hconvection) / ((1 / (hvapo + hconductive)) + (1 /
hconvective) + (1 / hconvection)))
   Pfm = VPf(Tfeedm, wfm)
   Ppm = VPp(Tpermeatm)
   Cfm = conc * Exp(flux / (rhofeed * Ksolute)) ' We want the bulk density
   wfm = Cfm * 58.5 / rhofeed * 100
   Jprev = flux
   flux = C_membrane * (Pfm - Ppm) * (101325 / 760)

   If flux <= 0 Then
      flux = 0
   End If
Loop
End Function
```

```
'FUNCTION WHICH CALCULATES THE REYNOLDS NUMBER

Function Re(rho, v, d, mu)

Re = (rho * v * d) / mu

End Function
```

```
'FUNCTION WHICH CALCULATES THE PRANDTL NUMBER

Function Pr(Cp, mu, k)
Pr = (Cp * mu) / k
End Function
```

```
'FUNCTION WHICH CALCULATES THE NUSSELT NUMBER

Function Nusselt(Reynolds, Prandl)

Dim f, Nuo, Nut, Nul, Nu1 As Double

f = 0.079 / (Reynolds ^ (0.25))
Nuo = 4.8
Nut = Nuo + (0.079 * ((f / 2) ^ (0.5)) * Reynolds * Prandl / ((1 + Prandl ^ 0.8) ^ (5 / 6)))
Nul = 3.657
Nu1 = Nul ^ 10 + ((Exp((2200 - Reynolds) / 365) / Nul ^ 2) + 1 / (Nut ^ 2)) ^ (-5)
Nusselt = Nu1 ^ (1 / 10)

End Function
```

```
'VAPOUR PRESSURE OF FEED SOLUTION
'Units: T[øC], w[weight percent], VPf[mmHg]

Function VPf(T, w)

If w = 0 Then
   VPf = 10 ^ (8.07131 - (1730.63 / (T + 233.426)))
Else
   VPf = (10 ^ (8.07131 - (1730.63 / (T + 233.426)))) * (1 - (wtf * 1000 / 58.5) / (wtf *
1000 / 58.5 + (1 - wtf) * 1000 / 18))
   'neglecting the concentration polarisation
End If


End Function
```

```
'VAPOUR PRESSURE OF PERMEATE SOLUTION
'UNITS: T[øC], VPp[mmHg]

Function VPp(T)

VPp = 10 ^ (8.07131 - (1730.63 / (T + 233.426)))

End Function
```

```
'HEAT OF VAPORIZATION OF WATER
'UNITS: Hvap[kJ/kg], T[øC]

Function Hvap(T)

Hvap = 2503.035313 - (2.430907 * T)

End Function
```

Appendix B

Experimental data

Hollow fibre module : Distilled water, Re feed=3000 (87L/min) and Re cooling=800 (40L/min)

Exp. Nb	Thot (°C)	Tcool(°C)	dT	Pv_hot (mmHg)	Pv_cool (mmHg)	dPv (mmHg)	Flow (g/min)	Flux (g/min.m2)	Re feed	Re cooling
10	33.3	26.4	6.9	38.3	25.7	12.5	6.62	3.31	3032	778
11	33.45	26	7.45	38.6	25.1	13.5	5.39	2.70	3041	771
12	33	25.4	7.6	37.6	24.3	13.4	5.84	2.92	3014	761
13	33.2	27.3	5.9	38.1	27.1	10.9	6.49	3.25	3026	794
14	32.6	21.3	11.3	36.8	18.9	17.9	8.91	4.46	2989	693
15	33.15	24.85	8.3	38.0	23.5	14.5	6.83	3.42	3023	752
16	33.1	24.95	8.15	37.8	23.6	14.2	7.30	3.65	3020	753
17	31.2	21.2	10	34.0	18.8	15.2	8.24	4.12	2905	691
18	31.2	21.3	9.9	34.0	18.9	15.1	8.33	4.17	2905	693
19	34	31	3	39.8	33.6	6.2	3.66	1.83	3074	858
20	28.8	23.4	5.4	29.6	21.5	8.1	3.84	1.92	2763	727
21	33	30.9	2.1	37.6	33.4	4.2	1.96	0.98	3014	856
22	28.7	22.6	6.1	29.4	20.5	8.9	3.77	1.89	2757	714
23	32.7	22.7	10	37.0	20.6	16.4	8.94	4.47	2995	716
24	34	23.2	10.8	39.8	21.3	18.5	8.82	4.41	3074	724
25	38.65	28.75	9.9	51.3	29.5	21.8	9.73	4.87	3362	819
43	33.2	25.7	7.5	38.1	24.7	13.4	5.70	2.85	3026	766
44	33.3	27.1	6.2	38.3	26.8	11.5	5.26	2.63	3032	790
45	31.7	22.3	9.4	35.0	20.1	14.8	7.51	3.76	2935	709
46	32.5	22.5	10	36.6	20.4	16.2	8.44	4.22	2983	712
47	33	30.3	2.7	37.6	32.3	5.3	2.77	1.39	3014	846
48	37.05	33.9	3.15	47.1	39.6	7.5	3.70	1.85	3262	910

Hollow fibre module : Distilled water, Re feed=1000 (30L/min) and Re cooling=540 (30L/min)

Exp. Nb	Thot (°C)	Tcool(°C)	dT	Pv_hot (mmHg)	Pv_cool (mmHg)	dPv (mmHg)	Flow (g/min)	Flux (g/min.m2)	Re feed	Re cooling
26	28.7	20	8.7	29.4	17.5	12.0	4.63	2.32	950	503
27	29.8	19.4	10.4	31.4	16.8	14.5	5.63	2.82	973	496
28	30.7	27.1	3.6	33.0	26.8	6.2	2.68	1.34	991	592
29	30.2	22.7	7.5	32.1	20.6	11.5	4.46	2.23	981	537
30	31	26.8	4.2	33.6	26.4	7.3	2.48	1.24	997	589
31	30.9	25.6	5.3	33.4	24.5	8.9	3.30	1.65	995	573
32	31.6	19.1	12.5	34.8	16.5	18.3	7.00	3.50	1010	493

Hollow fibre module : Distilled water, Re feed=1000 (30L/min) and Re cooling=750 (40L/min)

Exp. Nb	Thot (°C)	Tcool(°C)	dT	Pv_hot (mmHg)	Pv_cool (mmHg)	dPv (mmHg)	Flow (g/min)	Flux (g/min.m2)	Re feed	Re cooling
33	30.3	20.9	9.4	32.3	18.5	13.8	6.51	3.26	983	686
34	30.8	25	5.8	33.2	23.7	9.5	4.33	2.17	993	754
35	31.4	29.4	2	34.4	30.7	3.7	2.29	1.15	1006	830
36	30.4	23.3	7.1	32.5	21.4	11.1	5.39	2.70	985	726

Hollow fibre module : Distilled water, Re feed=3000 (87L/min) and Re cooling=400 (20L/min)

Exp. Nb	Thot (°C)	Tcool(°C)	dT	Pv_hot (mmHg)	Pv_cool (mmHg)	dPv (mmHg)	Flow (g/min)	Flux (g/min.m2)	Re feed	Re cooling
38	35.2	23.4	11.8	42.5	21.5	21.0	5.60	2.80	3148	363
39	35.6	27.4	8.2	43.5	27.3	16.2	4.24	2.12	3172	397
40	35.8	29.8	6	44.0	31.4	12.6	2.77	1.39	3185	418
41	36.9	28.1	8.8	46.7	28.4	18.3	4.40	2.20	3253	403
42	31.5	26.7	4.8	34.6	26.2	8.4	2.34	1.17	2941	395

Hollow fibre module : Distilled water, Re feed=670 (20L/min) and Re cooling=750 (40L/min)

Exp. Nb	Thot (°C)	Tcool(°C)	dT	Pv_hot (mmHg)	Pv_cool (mmHg)	dPv (mmHg)	Flow (g/min)	Flux (g/min.m2)	Re feed	Re cooling
50	31.3	24.3	7	34.2	22.7	11.5	5.05	2.53	669	742
51	30.8	20.5	10.3	33.2	18.0	15.2	6.90	3.45	662	680
52	31.8	29	2.8	35.2	30.0	5.2	2.80	1.40	676	823
53	31.6	27.2	4.4	34.8	27.0	7.8	3.56	1.78	673	792

Hollow fibre module : Distilled water, Re feed=1000 (30L/min) and Re cooling=400 (20L/min)

Exp. Nb	Thot (°C)	Tcool(°C)	dT	Pv_hot (mmHg)	Pv_cool (mmHg)	dPv (mmHg)	Flow (g/min)	Flux (g/min.m2)	Re feed	Re cooling
54	31.4	20.6	10.8	34.4	18.1	16.2	4.16	2.08	1006	340
55	31.3	19	12.3	34.2	16.4	17.8	4.75	2.38	1004	327
56	32.3	29.3	3	36.2	30.5	5.7	1.06	0.53	1024	414
57	32	27.5	4.5	35.6	27.5	8.1	2.09	1.05	1018	398
58	34	29	5	39.8	30.0	9.8	1.75	0.88	1060	411

Hollow fibre module : Distilled water, Re feed=400 (12L/min) and Re cooling=750 (40L/min)

Exp. Nb	Thot (°C)	Tcool(°C)	dT	Pv_hot (mmHg)	Pv_cool (mmHg)	dPv (mmHg)	Flow (g/min)	Flux (g/min.m2)	Re feed	Re cooling
59	34	30.7	3.3	39.8	33.0	6.8	2.43	1.22	424	853
60	32.2	25.8	6.4	36.0	24.8	11.1	4.51	2.26	409	768
61	32	24.3	7.7	35.6	22.7	12.9	5.86	2.93	407	742
62	31.9	21.5	10.4	35.4	19.2	16.2	6.82	3.41	406	696

Hollow fibre module : Distilled water, Re feed=3000 (87L/min) and Re cooling=1200 (60L/min)

Exp. Nb	Thot (°C)	Tcool(°C)	dT	Pv_hot (mmHg)	Pv_cool (mmHg)	dPv (mmHg)	Flow (g/min)	Flux (g/min.m2)	Re feed	Re cooling
63	31.85	27	4.85	35.3	26.7	8.6	6.70	3.35	2944	1183
64	33.2	28.2	5	38.1	28.6	9.5	7.68	3.84	3026	1214
65	35.7	30.8	4.9	43.7	33.2	10.5	8.53	4.27	3179	1282
66	28.9	25.2	3.7	29.8	24.0	5.8	4.42	2.21	2769	1137

Hollow fibre module : Distilled water, Re feed=3000 (87L/min) and Re cooling=2200 (110L/min)

Exp. Nb	Thot (°C)	Tcool(°C)	dT	Pv_hot (mmHg)	Pv_cool (mmHg)	dPv (mmHg)	Flow (g/min)	Flux (g/min.m2)	Re feed	Re cooling
67	28.9	26.7	2.2	29.8	26.2	3.6	3.70	1.85	2769	2155
68	28.9	25.7	3.2	29.8	24.7	5.1	5.25	2.63	2769	2108
69	31.3	28.1	3.2	34.2	28.4	5.8	6.17	3.09	2911	2221
70	33.6	30.3	3.3	38.9	32.3	6.6	6.90	3.45	3050	2327

Hollow fibre module : Distilled water, Re feed=3000 (87L/min) and Re cooling=1600 (80L/min)

Exp. Nb	Thot (°C)	Tcool(°C)	dT	Pv_hot (mmHg)	Pv_cool (mmHg)	dPv (mmHg)	Flow (g/min)	Flux (g/min.m2)	Re feed	Re cooling
71	30	27	3	31.7	26.7	5.1	5.00	2.50	2834	1577
72	29.7	25.8	3.9	31.2	24.8	6.4	6.37	3.19	2816	1536
73	32.5	28.7	3.8	36.6	29.4	7.1	7.31	3.66	2983	1636
74	29.7	27.7	2	31.2	27.8	3.4	3.05	1.53	2816	1601

Hollow fibre module : 3.4 wt.% NaCl, Re feed=3000 (87L/min) and Re cooling=2300 (110L/min)

Exp. Nb	Thot (°C)	Tcool(°C)	dT	Pv_hot (mmHg)	Pv_cool (mmHg)	dPv (mmHg)	Flow (g/min)	Flux (g/min.m2)	Re feed	Re cooling
77	33.2	30.05	3.15	38.1	31.8	6.2	6.05	3.03	2934	2315
78	35.2	32	3.2	42.5	35.6	7.0	7.17	3.59	3053	2410
79	36.9	33.75	3.15	46.7	39.2	7.4	7.35	3.68	3155	2496
80	30.2	27.1	3.1	32.1	26.8	5.3	4.84	2.42	2760	2174

Tubular module : Distilled water, Re feed = 3000 (20L/min) and Re cooling = 1150 (20L/min)

Exp. Nb	Thot (°C)	Tcool(°C)	dT	Pv_hot (mmHg)	Pv_cool (mmHg)	dPv (mmHg)	Flux (g/min.m2)	model (g/min)	(Fmod-Fexp)/Fmod*100	Re feed	Re cooling
T1	47.1	39	8.1	79.8	52.3	27.5	7.61	7.96	4.4	3226	1437
T2	45.4	35.1	10.3	73.2	42.3	30.9	9.42	8.96	-5.1	3134	1334
T3	45.5	35.6	9.9	73.6	43.5	30.1	8.94	8.72	-2.5	3139	1347
T4	45.4	35.5	9.9	73.2	43.2	29.9	8.66	8.68	0.2	3134	1344
T5-1	45.5	35.2	10.3	73.6	42.5	31.0	9.03	9	-0.3	3139	1336
T5-2	35.9	26.9	9.0	44.2	26.5	17.7	5.12	5.01	-2.2	2635	1126
T6-1	35.9	27.1	8.8	44.2	26.8	17.4	4.99	4.92	-1.4	2635	1131
T6-2	43.4	33.4	10.0	66.0	38.5	27.5	8.16	7.96	-2.5	3026	1290
T7	39.8	22.8	17.0	54.6	20.7	33.9	10.02	9.77	-2.6	2836	1027
T8	39.7	23.4	16.3	54.3	21.5	32.8	9.12	9.46	3.6	2831	1041
T9	39.8	23.6	16.2	54.6	21.8	32.8	9.44	9.47	0.3	2836	1046
T10	32.2	18.2	14.0	36.0	15.6	20.4	5.85	5.68	-3.0	2448	920
T11	32.2	17.6	14.6	36.0	15.0	20.9	5.94	5.85	-1.5	2448	906
T12	26.1	14.2	11.9	25.3	12.1	13.2	3.75	3.6	-4.2	2152	830
T13	41.2	24.6	16.6	58.8	23.1	35.7	10.86	10.35	-4.9	2910	1070

Appendix C

Calculation samples

Theoretical models calculations

For the following experimental conditions (experiment Tubular-10) and membrane characteristics :

- T_{feed}=305.35 K, feed temperature
- $T_{cooling}$=291.35, cooling temperature
- ΔP_v=2720 Pa, vapour pressure difference
- P=101325 Pa, pore pressure
- d=0.2 μm, pore diameter
- ε=0.75, membrane porosity
- τ=1.3, membrane tortuosity
- δ_m=0.4 mm, membrane thickness (hollow fibre unit)
- μ=1.85*10^{-5} Pa.s, viscosity of water vapour at 30°C [23]

Water molecules mean free path :

$$\lambda = 3\mu/P\ [\pi RT/(8M)]^{1/2}$$

$$\lambda = 3*1.85*10^{-5}/101325*[\pi*8.314*305.35/8/(18*10^{-3})]^{1/2}$$

$$\lambda \cong 0.13\ \mu m$$

Diffusion coefficient [23] :

$$D_{wa} = 0.01013\ T^{1.75}\ (1 / M_w + 1 / M_a)^{1/2} / [P\ (v_w^{1/3} + v_a^{1/3})^2]$$

$$D_{wa} = 0.01013*305.35^{1.75}*(1/18+1/28.86)^{1/2} / [101325*(20.1^{1/3} + 12.7^{1/3})^2]$$

$$D_{wa} \cong 2.62*10^{-5}\ m^2/s$$

Knudsen diffusion :

$J = 2/3\ r\varepsilon / \tau\ [8M/(\pi RT)]^{1/2}\ \Delta P/\delta_m$

$J = 2/3*0.1*10^{-6}*0.75/1.3*[8*18*10^{-3}/8.314/305.35/\pi]^{1/2} * 2720/(0.4*10^{-3})$

$J \cong 1.11*10^{-3}\ kg/m^2.s$

Molecular diffusion :

$N_A = \varepsilon D_{AB} P \ln[(P-P_{v2})/(P-P_{v1})] / (RT\delta_m\tau)$

$N_A = 0.75*2.62*10^{-5}*101325*\ln[(760-15.6)/(760-36)]/8.314/305.35/1.3/(0.4*10^{-3})$

$N_A \cong 0.042\ mol/m^2.s$

Hagen-Poiseuille viscous flow :

$J = r^2\varepsilon M P \Delta P_v / (8\mu RT\delta_m\tau)$

$J = 1/8*(0.1*10^{-6})^2*0.75/1.3/1.85*10^{-5}*18*10^{-3}*101325/8.314/305.35*2720/(0.4*10^{-3})$

$J \cong 1.90*10^{-4}\ kg/m^2.s^{-1}$